Equalization of the Correlated Additive Gaussian Noises on the Wireless Links of Sensor Networks

by

Sou-Yu Cheng

Thesis submitted to the Institute of Communications Engineering
National Chiao Tung University, Taiwan
in partial fulfillment of the requirements
for the degree of Master of Science
2006

Advisory Committee:

Professor Po-Ning Chen, Advisor
Professor Yunghsiang S. Han
Professor Wern-Ho Sheen
Professor Tsang-Yi Wang

中文摘要

有鑑於設置在惡劣環境中的無線感測器的高故障率對於無線感測器網路的系統偵測正確率有極大的影響，最近已提出運用錯誤更正碼技術之分散式分類資訊整合方法 (Distributed Classification Fusion using Error Correcting Codes or DCFECC) 作為解決方式。這個方法可在有限的電池能量支援下，提供相當高的系統容錯能力。之前有關運用錯誤更正碼技術之分散式分類資訊整合方法的研究，都是在無線通道雜訊互相獨立且相同分佈 (independent and identically distributed) 的假設下進行。在這篇論文中，我們將此假設進一步延伸，討論在空間雜訊相關的情況下，運用錯誤更正碼技術之分散式分類資訊整合方法的實現可行性。簡言之，我們的系統包含通道估計及等化，與使用最小歐式距離整合規則 (Minimum-Euclidean Distance fusion rule or MED fusion rule)。實驗顯示，此規則在空間相關的無線通道雜訊環境，確實具有不錯的容錯能力。另外，我們也提供了一個簡單的碼搜尋準則，可在低運算複雜度之下，完成碼矩陣的設計。模擬的結果顯示，最小歐式距離整合規則在白色高斯雜訊通道、空間相關雜訊通道、以及互相獨立但不同分佈的雜訊通道當中，都展現對抗故障感測器的高容錯能力。

ABSTRACT

Distributed classification fusion using error correcting codes (DCFECC) has recently been proposed for wireless sensor networks operating in a harsh environment. It has been shown to provide a considerable fault-tolerance capability against unexpected sensor faults under limited energy support. In this thesis, we extend the DCFECC approach by relaxing the assumption of independently and identically distributed wireless link noises to correlated ones. Through channel estimation and equalization, we obtain a fault-tolerant minimum Euclidean distance (MED) fusion rule suitable for use under correlated wireless link noises. A simple code search criterion is also proposed to make the code matrix design feasible with acceptable computational complexity. Simulation results show that the proposed MED fusion rule truly achieves the desired robustness against sensor faults under the simulated AWGN channels, spatially correlated channels and non-identical uncorrelated channels.

ACKNOWLEDGMENTS

I would like to thank everyone who helps me complete this thesis.

To my advisor, Professor Chen, it is your patient instruction and brilliant guidance to make this thesis possible. I learn a lot from you. It is my pleasure to be advised by you.

To Professors Han and Wang, thanks for your opinions and explicit explanations in our frequent meetings. You help me understand more about the research topic.

To my lab-mates and research partners in NTPU, you always listen to my problems, give me useful advises, and encourage me when I am confused or depressed. I really appreciate it.

In the end, I would like to dedicate this thesis to my family, for their love and support all the time.

TABLE OF CONTENTS

LIST OF TABLES

LIST OF FIGURES

Chapter 1

Introduction

Recent advance in microprocessor, radio, and battery technology has enabled the development of low-cost wireless sensors. These tiny sensor nodes can not only detect the status of target objects, process the information, but also transmit the data to a fusion center through wireless noisy links. By collecting information from a large number of distributed sensor nodes, wireless sensor networks (WSNs) can be deployed for many applications, e.g., environmental monitoring, battle field surveillance, and health care maintenance [1], [2], [3], [4], [5], [6]. The ability to classify the target objects is usually the fundamental requirement.

In WSNs, the wireless sensor nodes are typically battery-powered and made by economical techniques. This makes energy efficiency and fault-tolerance capability becoming the important issues for WSN system design. Due to the limitation on the communication bandwidth in wireless links and limited energy consumption at local sensors, it is necessary for each local sensor to compress the raw observation data before transmitting it to the fusion center. Additionally, when being deployed in a harsh environment,

these low-cost sensors may prone to be blocked or damaged, which results in unexpected sensor faults.

In order to achieve the desired robustness against sensor faults under limited energy support, a distributed classification fusion approach using error correcting codes (DCFECC) has been proposed in [7]. In the DCFECC approach, Each local sensor employs a decision rule based on a pre-designed code matrix and sends one-bit information to the fusion. The fusion center then makes the final classification decision based on the binary received vector by performing the minimum Hamming distance fusion.

Unlike the conventional approach that employs the optimal MAP rule, the minimum Hamming distance fusion rule is shown to be able to provide enough distance between all the decision regions corresponding to different hypotheses by using the code matrix, and hence, can achieve the desired robustness against sensor failures. In other words, when sensor faults occur, the resultant Hamming distance is less affected by the outputs of those damaged sensors. As a result, the DCFECC approach gives good fault-tolerance capability in the presence of sensor faults.

In this work, we further extend the DCFECC approach by relaxing the assumption of independently and identically distributed wireless link noises. Within a wireless sensor network, the information from a great quantity of sensors is usually collected inside a small space. Thus, the assumption of

independent link noises may not be reasonable. It is therefore necessary to consider the wireless link channel with correlated noises.

As contrary to the minimum Hamming distance fusion employed in [7], we propose to use the minimum Euclidean distance (MED) fusion instead for a soft-decision fusion is assumed in our WSNs. Further, the technology of channel estimation and equalization is added to compensate the additive correlated link noises. With the help of the pre-sent training sequence, the maximum-likelihood (ML) estimator of channel covariance matrix is derived. Afterwards, through the whitening technique, we modify the MED rule according to the estimated channel covariance matrix, and finally get the fault-tolerant fusion rule suitable for use under correlated wireless link noises.

As anticipated, the classification performance of the DCFECC approach is strongly related to the chosen code matrix. However, due to the very large amount of sensors, exhaustive search for an optimal code matrix is computationally intensive and unaffordable. How to find a good code matrix within a reasonable algorithmic complexity also becomes a research subject in WSNs. Two usual code design algorithms, namely the cyclic column replacement approach and the simulated annealing, have been tried in [7], [8]. In this thesis, we propose to employ a simple union bound as a code search criterion to be minimized. In terms of the MED fusion rule, and by assum-

ing additive white Gaussian link noises (AWGN), the union bound of the fusion error probability can be expressed in a refined form. Using this criterion, code matrix search becomes feasible with acceptable computational complexity.

Performance of the proposed minimum Euclidean distance fusion rule is examined through plenty of simulations. As anticipated, the simulation results under AWGN wireless link noises show that the MED fusion rule is more robust against sensor faults than the MAP fusion rule. Further, by observing the simulation results under several different channel models, the channel effect upon the system performance will also be remarked.

This thesis is organized in the following fashion. The system model is described in Chapter 2. The MAP and the fault-tolerant minimum Euclidean distance fusion rules are introduced in Chapter 3, followed by the modified fusion rule considering correlated wireless link noises. In Chapter 4, the channel estimation and equalization technique is presented. In Chapter 5, we propose a code search criterion acquired by the union bound we derived. Simulations under several channel models are presented and remarked in Chapter 6. Conclusion is given in Chapter 7.

Chapter 2

System Model

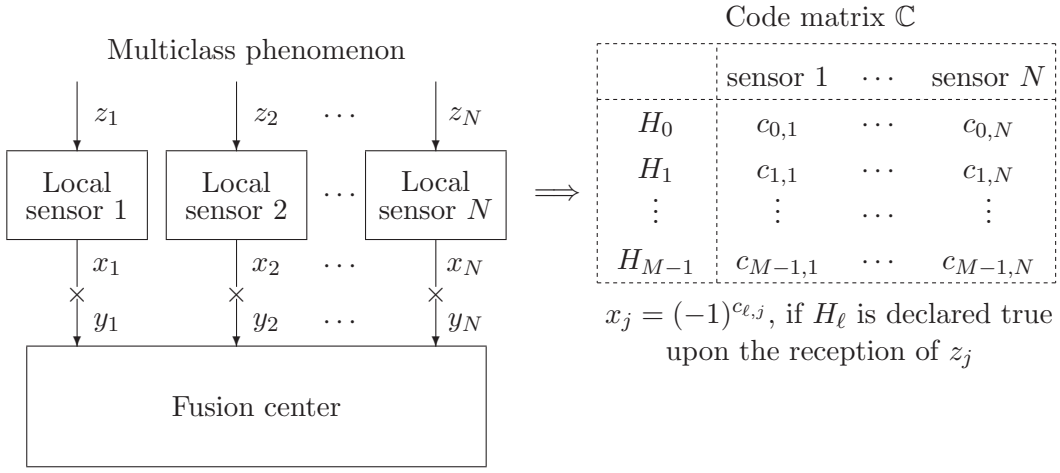

Figure 2.1: System model.

Figure 2.1 depicts the distributed M-ary classification system considered in this thesis.

As shown in this figure, we assume that the local sensor observations $\{z_j\}_{j=1}^N$ are conditionally independent given each hypothesis, where N is the number of sensors. Also assume that each sensor makes a local classification decision uncooperatively using its own decision rule based on its own observation z_j. Denote by $h_{\ell|i}^{(j)}$ the probability of classifying H_ℓ given that

H_i is the true hypothesis at sensor j. Moreover, the prior probability of each hypothesis is assumed equal.

On the right-hand-side of Fig. 2.1 indicates a pre-specified code matrix $\mathbb{C}$. It is an $M \times N$ matrix with element $c_{\ell,j} \in \{0, 1\}$, where $\ell = 0, \ldots, M-1$ and $j = 1, \ldots, N$. Each hypothesis H_ℓ is associated with a row in the code matrix, and each column vector in $\mathbb{C}$ provides the local binary outputs corresponding to the locally classified hypotheses at the respective sensor. So to speak, if sensor j makes a local classification decision H_ℓ, it will transmit $x_j = (-1)^{c_{\ell,j}}$ to the fusion center. The code matrix can be designed based on the misclassification error criterion, which will be discussed in Chapter 5.

The communication channel between sensors and fusion center is assumed to be a spatially correlated additive Gaussian channel. To be specific, received vector $\boldsymbol{y}$ is given by

$$\boldsymbol{y} = \boldsymbol{x} + \mathbb{T}\boldsymbol{n},$$

where $\boldsymbol{y} = (y_1, \ldots, y_N) \in \Re^N$, $\boldsymbol{x} = (x_1, \ldots, x_N) \in \{-1, 1\}^N$, and $\boldsymbol{n} = (n_1, \ldots, n_N) \in \Re^N$ is i.i.d. Gaussian distributed with zero mean and unit marginal variance. As a result, the covariance matrix of the correlated noises is given by $\mathbb{C} = E[\mathbb{T}\boldsymbol{n}(\mathbb{T}\boldsymbol{n})^T] = \mathbb{T}\mathbb{T}^T$, and the probability of receiving $\boldsymbol{y}$ given that $\boldsymbol{x}$ is transmitted is equal to:

$$\Pr(\boldsymbol{y}|\boldsymbol{x}) = \frac{1}{(2\pi)^{\frac{m}{2}}|\mathbb{C}|^{\frac{1}{2}}} \exp\left\{-\frac{1}{2}(\boldsymbol{y}-\boldsymbol{x})^T\mathbb{C}^{-1}(\boldsymbol{y}-\boldsymbol{x})\right\},$$

provided that $\mathbb{C}$ is invertible. In the end, a fusion rule is employed to obtain the multiclass decision.

Chapter 3

Soft-Decision Fusion Rule

3.1 Optimal MAP fusion rule under AWGN wireless link noises

The MAP fusion rule favors the decision $H_{\hat{i}}$ under the premise that upon the reception of $\boldsymbol{y}$, the posterior probability $\Pr(H_{\hat{i}}|\boldsymbol{y})$ is maximized. It can be derived as:

$$\begin{aligned}
\hat{i} &= \arg \max_{0\le\ell\le M-1} \Pr(H_\ell|\boldsymbol{y}) \\
&= \arg \max_{0\le\ell\le M-1} \Pr(\boldsymbol{y}|H_\ell), \text{ due to equally probabable hypotheses} \\
&= \arg \max_{0\le\ell\le M-1} \sum_{\boldsymbol{x}\in\{-1,1\}^N} \Pr(\boldsymbol{x},\boldsymbol{y}|H_\ell) \\
&= \arg \max_{0\le\ell\le M-1} \sum_{\boldsymbol{x}\in\{-1,1\}^N} \Pr(\boldsymbol{x}|H_\ell)\Pr(\boldsymbol{y}|\boldsymbol{x},H_\ell) \\
&= \arg \max_{0\le\ell\le M-1} \sum_{\boldsymbol{x}\in\{-1,1\}^N} \Pr(\boldsymbol{x}|H_\ell)\Pr(\boldsymbol{y}|\boldsymbol{x}), \text{ since } \Pr(\boldsymbol{y}|\boldsymbol{x},H_\ell)=\Pr(\boldsymbol{y}|\boldsymbol{x}) \\
&= \arg \max_{0\le\ell\le M-1} \sum_{\boldsymbol{x}\in\{-1,1\}^N} \left(\prod_{j=1}^{N}\Pr(x_j|H_\ell)\right)\Pr(\boldsymbol{y}|\boldsymbol{x}),
\end{aligned}$$

where the last step follows since the local observations are assumed spatially independent given each hypothesis, and x_j is determined independently across sensors. Here, we abuse the notation $\Pr(\cdot)$ to denote either the

probability mass function (pmf) or the probability density function (pdf), depending on whether the support is discrete or continuous. For example, $\Pr(H_\ell|\boldsymbol{y})$ denotes a probability mass function as the image of H_ℓ is discrete, while $\Pr(\boldsymbol{y}|H_\ell)$ is a probability density function as $\boldsymbol{y}$ belongs to a continuous domain. Notably, $\Pr\{x_j = -1|H_i\} = \sum_{\ell=0}^{M-1} c_{\ell,j} h_{\ell|i}^{(j)}$, and $\Pr\{x_j = 1|H_i\} = \sum_{\ell=0}^{M-1}(1-c_{\ell,j})h_{\ell|i}^{(j)}$. Taking $\Pr\{\boldsymbol{y}|\boldsymbol{x}\}$ due to AWGN wireless link noises (namely, $\mathbb{T}$ is a diagonal matrix with equal diagonal $\sigma = \sqrt{N_0/2}$) into the above derivation, we further obtain:

$$\begin{aligned}
\hat{i} &= \arg \max_{0\le\ell\le M-1} \sum_{\boldsymbol{x}\in\{-1,1\}^N} \left(\prod_{j=1}^{N} \Pr(x_j|H_\ell)\right) \left(\prod_{j=1}^{N} \frac{1}{\sqrt{2\pi}\sigma} \exp\left\{-\frac{(y_j-x_j)^2}{2\sigma^2}\right\}\right) \\
&= \arg \max_{0\le\ell\le M-1} \sum_{\boldsymbol{x}\in\{-1,1\}^N} \left(\prod_{j=1}^{N} \Pr(x_j|H_\ell) \exp\left\{-\frac{(y_j-x_j)^2}{2\sigma^2}\right\}\right) \\
&= \arg \max_{0\le\ell\le M-1} \prod_{j=1}^{N} \left(\sum_{x_j\in\{-1,1\}} \Pr(x_j|H_\ell) \exp\left\{-\frac{(y_j-x_j)^2}{2\sigma^2}\right\}\right) \\
&= \arg \max_{0\le\ell\le M-1} \prod_{j=1}^{N} \left(\sum_{x_j\in\{-1,1\}} \Pr(x_j|H_\ell) \exp\left\{\frac{x_j y_j}{\sigma^2}\right\}\right) \\
&= \arg \max_{0\le\ell\le M-1} \sum_{j=1}^{N} \log\left[1 - \left(1 - e^{-\frac{2y_j}{\sigma^2}}\right)\left(\sum_{i=0}^{M-1} c_{i,j} h_{i|\ell}^{(j)}\right)\right]. \qquad (3.1)
\end{aligned}$$

This is the expression for the optimal MAP fusion rule under i.i.d. zero-mean link noise $\mathbb{T}\boldsymbol{n}$ with marginal variance $\sigma^2 = N_0/2$.

3.2 Suboptimal minimum Euclidean distance fusion rule under AWGN wireless link noises

It is apparent from the derivation in the previous section that the optimal MAP fusion rule relies heavily on the posterior probability $\Pr(H_\ell|\boldsymbol{y})$. However, in situation when some faulty sensors send untrustworthy outputs (that are generated according to some rule different from the mutually agreed one between the local sensor and fusion center), the true posterior probability will deviate from the $\Pr(H_\ell|\boldsymbol{y})$ used in the MAP rule. Such a mismatch in $\Pr(H_\ell|\boldsymbol{y})$ may considerably degrade the classification performance. This arises the demand of an alternative fusion rule that is less sensitive to sensor failure.

One potential candidate fusion rule that is robust to sensor faults is the minimum Euclidean distance fusion rule. Although it is only suboptimal when no sensor faults occur, the minimum Euclidean distance fusion rule is robust to sensor failure since the Euclidean distance is less affected by untrustworthy sensor outputs. It is worth mentioning that when the local classification is adequately accurate, the suboptimal minimum Euclidean distance fusion rule performs close to the optimal MAP fusion rule in a sensor-fault-free environment. Specifically, if

$$\Pr\{x_j = (-1)^{c_{\ell,j}}|H_\ell\} \gg \Pr\{x_j \neq (-1)^{c_{\ell,j}}|H_\ell\},$$

then $\Pr\{x_j = (-1)^{c_{\ell,j}}|H_\ell\} \approx 1$ and $\Pr\{x_j \neq (-1)^{c_{\ell,j}}|H_\ell\} \approx 0$, and

$$\begin{aligned}
\hat{i} &\approx \arg \max_{0\leq\ell\leq M-1} \prod_{j=1}^{N} \exp\left\{-\frac{(y_j-(-1)^{c_{\ell,j}})^2}{2\sigma^2}\right\} \\
&= \arg \min_{0\leq\ell\leq M-1} \sum_{j=1}^{N} (y_j-(-1)^{c_{\ell,j}})^2 \\
&= \arg \min_{0\leq\ell\leq M-1} \|\boldsymbol{y}-(-1)^{\boldsymbol{c}_\ell}\|^2, \qquad (3.2)
\end{aligned}$$

where $\boldsymbol{c}_\ell \triangleq (c_{\ell,1}, c_{\ell,2}, \ldots, c_{\ell,N})$ denotes the row of $\mathbb{C}$ corresponding to the hypothesis H_ℓ.

3.3 Fault-tolerant minimum Euclidean distance fusion rule under spatially correlated link noises

Under spatially correlated wireless link noises, $\mathbb{T}$ is no longer a diagonal matrix. Let $\mathbb{W}$ be the whitening matrix with respect to $\mathbb{T}$.[1] Then, after whitening, we transform the originally spatially correlated system into one with uncorrelated noises as:

$$\mathbb{W}\boldsymbol{y} = \mathbb{W}\boldsymbol{x} + \mathbb{W}\mathbb{T}\boldsymbol{n}.$$

[1]The inverse matrix of $\mathbb{T}$ may not exist in general. However, the whitening matrix $\mathbb{W}$ with respect to colored noise $\mathbb{T}\boldsymbol{n}$ always exist. Specifically, $\mathbb{W} = \Delta^{-1}\mathbb{B}^T$, where nonnegative definite $\mathbb{C} = \mathbb{T}\mathbb{T}^T$ can be represented as $\mathbb{B}\Lambda\mathbb{B}^T$ for $\mathbb{B}$ orthogonal and Λ diagonal with nonnegative entries, and Δ is a diagonal matrix with $\Delta_{kk} = \Lambda_{kk}^{1/2}$ if $\Lambda_{kk} > 0$ and $\Delta_{kk} = 1$ if $\Lambda_{kk} = 0$.

Then, the minimum Euclidean distance fusion rule under spatially correlated link noises is given by:

$$\begin{aligned}
\hat{i} &= \arg \min_{0 \le \ell \le M-1} \|\mathbb{W}\boldsymbol{y} - \mathbb{W}(-1)^{\boldsymbol{c}_\ell}\|^2 \\
&= \arg \min_{0 \le \ell \le M-1} \|\mathbb{W}\left[\boldsymbol{y} - (-1)^{\boldsymbol{c}_\ell}\right]\|^2 \\
&= \arg \min_{0 \le \ell \le M-1} \left[\boldsymbol{y} - (-1)^{\boldsymbol{c}_\ell}\right]^T \mathbb{W}^T\mathbb{W}\left[\boldsymbol{y} - (-1)^{\boldsymbol{c}_\ell}\right].
\end{aligned}$$

If $\mathbb{C} = \mathbb{T}\mathbb{T}^T$ is invertible, then

$$\hat{i} = \arg \min_{0 \le \ell \le M-1} \left[\boldsymbol{y} - (-1)^{\boldsymbol{c}_\ell}\right]^T \mathbb{C}^{-1}\left[\boldsymbol{y} - (-1)^{\boldsymbol{c}_\ell}\right]. \tag{3.3}$$

Chapter 4

Estimation and Equalization of Parallel Wireless Link Channels

The fusion rule in (3.3) requires the knowledge of the noise covariance matrix $\mathbb{C}$. However, this information may not be available at the fusion center in practice. Thus, it may be necessary to estimate $\mathbb{C}$ beforehand.

A common approach for channel estimation is the use of the training sequence. In our system setting, K training bits are initially and sequentially sent to the fusion center at each sensor. Then, the fusion center makes an estimate of $\mathbb{C}$ based upon the K training vectors it receives in sequence. In notations, these training vectors are denoted by $\boldsymbol{u}_1$, $\boldsymbol{u}_2$, ..., $\boldsymbol{u}_K$, where $\boldsymbol{u}_j = (u_{j,1}, u_{j,2}, \ldots, u_{j,N})$, and $u_{j,m} \in \{-1, 1\}$ is the training bit sent by sensor m at time j.

As $\boldsymbol{u}_1$, $\boldsymbol{u}_2$, ..., $\boldsymbol{u}_K$ are known to the fusion center, the channel estimation problem becomes to estimate $\mathbb{C} = \mathbb{T}\mathbb{T}^T$ upon the reception of $\boldsymbol{y}_k = \boldsymbol{u}_k + \mathbb{T}\boldsymbol{n}_k$ for $1 \leq k \leq K$. It can be shown that in such case, the

maximum-likelihood (ML) estimator of $\mathbb{C}$ is equal to

$$\hat{\mathbb{C}}_{ML} = \frac{1}{K}\sum_{k=1}^{K}(\boldsymbol{y}_k - \boldsymbol{u}_k)(\boldsymbol{y}_k - \boldsymbol{u}_k)^T, \tag{4.1}$$

for which the detail is given below. We can then apply $\hat{\mathbb{C}}_{ML}$ in fusion rule (3.3) to obtain a decision on the true hypothesis.

It remains to prove (4.1). Under the assumption that the channel covariance matrix $\mathbb{C}$ is nonsingular, we obtain that

$$\Pr(\boldsymbol{y}_1, \cdots, \boldsymbol{y}_K | \boldsymbol{u}_1, \cdots, \boldsymbol{u}_K) = \frac{1}{(2\pi)^{\frac{NK}{2}}|\mathbb{C}|^{\frac{K}{2}}} \exp\left\{-\frac{1}{2}\sum_{k=1}^{K}(\boldsymbol{y}_k - \boldsymbol{u}_k)^T\mathbb{C}^{-1}(\boldsymbol{y}_k - \boldsymbol{u}_k)\right\}.$$

Then the ML estimate can be written as:

$$\begin{aligned}\hat{\mathbb{C}}_{ML} &= \arg\max_{\mathbb{C}} \Pr(\boldsymbol{y}_1, \cdots, \boldsymbol{y}_K | \boldsymbol{u}_1, \cdots, \boldsymbol{u}_K) \\ &= \arg\max_{\mathbb{C}} L(\mathbb{C}),\end{aligned}$$

where

$$L(\mathbb{C}) \triangleq |\mathbb{C}|^{-K/2} \exp\left\{-\frac{1}{2}\sum_{k=1}^{K}(\boldsymbol{y}_k - \boldsymbol{u}_k)^T\mathbb{C}^{-1}(\boldsymbol{y}_k - \boldsymbol{u}_k)\right\}.$$

Function $L(\mathbb{C})$ can be re-expressed as:

$$\begin{aligned}L(\mathbb{C}) &= |\mathbb{C}|^{-K/2} \exp\left\{-\frac{1}{2}\sum_{k=1}^{K}\mathrm{tr}\left((\boldsymbol{y}_k - \boldsymbol{u}_k)^T\mathbb{C}^{-1}(\boldsymbol{y}_k - \boldsymbol{u}_k)\right)\right\} \\ &= |\mathbb{C}|^{-K/2} \exp\left\{-\frac{1}{2}\sum_{k=1}^{K}\mathrm{tr}\left((\boldsymbol{y}_k - \boldsymbol{u}_k)(\boldsymbol{y}_k - \boldsymbol{u}_k)^T\mathbb{C}^{-1}\right)\right\} \qquad (4.2) \\ &= |\mathbb{C}|^{-K/2} \exp\left\{-\frac{1}{2}\mathrm{tr}\left(\sum_{k=1}^{K}(\boldsymbol{y}_k - \boldsymbol{u}_k)(\boldsymbol{y}_k - \boldsymbol{u}_k)^T\mathbb{C}^{-1}\right)\right\} \\ &= |\mathbb{C}|^{-K/2} \exp\left\{-\frac{1}{2}\mathrm{tr}\left(\mathbb{S}\mathbb{C}^{-1}\right)\right\}, \qquad (4.3)\end{aligned}$$

where (4.2) holds due to cyclic property of the matrix trace operation, and

$$\mathbb{S} \triangleq \sum_{k=1}^{K} (\boldsymbol{y}_k - \boldsymbol{u}_k)(\boldsymbol{y}_k - \boldsymbol{u}_k)^T.$$

Further assume that the symmetric $\mathbb{S}$ is positive-definite; hence, it has a unique positive-definite symmetric square root $\mathbb{S}^{1/2}$. This reduces (4.3) to:

$$\begin{aligned} L(\mathbb{C}) &= |\mathbb{C}|^{-K/2} \exp\left\{-\frac{1}{2}\text{tr}\left(\mathbb{S}^{1/2}\mathbb{C}^{-1}\mathbb{S}^{1/2}\right)\right\} \\ &= |\mathbb{S}|^{-K/2}|\mathbb{D}|^{K/2} \exp\left\{-\frac{1}{2}\text{tr}(\mathbb{D})\right\} \\ &= |\mathbb{S}|^{-K/2}\left(\prod_{i=1}^{N}\lambda_i\right)^{K/2} \exp\left(-\frac{1}{2}\sum_{i=1}^{N}\lambda_i\right), \end{aligned}$$

where $\mathbb{D} \triangleq \mathbb{S}^{1/2}\mathbb{C}^{-1}\mathbb{S}^{1/2}$, and $\lambda_1, \cdots, \lambda_N$ are the eigenvalues of $\mathbb{D}$. The optimal $\lambda_1, \cdots, \lambda_N$ that maximize $L(\mathbb{C})$ are the ones that $\lambda_1 = \cdots = \lambda_N = K$, which makes $\hat{\mathbb{D}}_{ML} = K \cdot \mathbb{I}_N$, where $\mathbb{I}_N$ is the $N \times N$ identity matrix. Finally, from $\hat{\mathbb{D}}_{ML} = \mathbb{S}^{1/2}\hat{\mathbb{C}}_{ML}^{-1}\mathbb{S}^{-1/2}$, we get that the ML estimator of the channel covariance matrix is:

$$\begin{aligned} \hat{\mathbb{C}}_{ML} &= \mathbb{S}^{1/2}\hat{\mathbb{D}}_{ML}^{-1}\mathbb{S}^{1/2} = \mathbb{S}^{1/2}\left(\frac{1}{K}\cdot\mathbb{I}_N\right)\mathbb{S}^{1/2} \\ &= \frac{\mathbb{S}}{K} \\ &= \frac{1}{K}\sum_{k=1}^{K}(\boldsymbol{y}_k - \boldsymbol{u}_k)(\boldsymbol{y}_k - \boldsymbol{u}_k)^T. \end{aligned}$$

Chapter 5

Code Search Based on Union Bound

The code matrix employed in our wireless sensor network plays an important role in the determination of system performance. It specifies not only how each sensor makes its local binary decision, but also how the fusion center manipulates the information collected from sensors. Thus, the design methodology of the code matrix is essential.

The underlying design objective of a good code matrix is to have the fusion system exhibit good performance in both fault-free and faulty situations. On the one hand, the minimum pairwise Hamming distance among codewords in the code matrix should be large so that the system can tolerate more sensor faults under faulty situation. On the other hand, the code matrix should achieve good misclassification error under fault-free situation, which seemingly favors the minimum-fusion-error criterion; however, the minimum-fusion-error criterion is too complex as a target code search criterion to be minimized even for a sensor network with moderate number of sensors. We therefore propose in this thesis to employ the simple union bound as a code search criterion to be minimized, subject to a minimum pairwise Hamming

distance constraint.

Using (3.2) as the fusion rule under AWGN wireless link noises, we derive the probability of fusion error given that H_i is the true hypothesis as:

$$\begin{aligned}
\Pr[\text{error}|H_i] &\leq \Pr\left\{ \|\boldsymbol{y} - (-1)^{\boldsymbol{c}_i}\| \geq \min_{0\leq \ell \leq M-1, \ell \neq i} \|\boldsymbol{y} - (-1)^{\boldsymbol{c}_\ell}\| \middle| H_i \right\} \\
&\leq \sum_{0\leq \ell \leq M-1, \ell \neq i} \Pr\left\{ \|\boldsymbol{y} - (-1)^{\boldsymbol{c}_i}\|^2 \geq \|\boldsymbol{y} - (-1)^{\boldsymbol{c}_\ell}\|^2 \middle| H_i \right\} \\
&= \sum_{0\leq \ell \leq M-1, \ell \neq i} \Pr\left\{ \sum_{j=1}^{N} \left[(y_j - (-1)^{c_{i,j}})^2 - (y_j - (-1)^{c_{\ell,j}})^2 \right] \geq 0 \middle| H_i \right\} \\
&= \sum_{0\leq \ell \leq M-1, \ell \neq i} \Pr\left\{ \sum_{j=1}^{N} y_j \left[(-1)^{c_{\ell,j}} - (-1)^{c_{i,j}} \right] \geq 0 \middle| H_i \right\} \\
&= \sum_{0\leq \ell \leq M-1, \ell \neq i} \Pr\left\{ \sum_{\{j \,:\, c_{\ell,j}=0, c_{i,j}=1\}} y_j - \sum_{\{j \,:\, c_{\ell,j}=1, c_{i,j}=0\}} y_j \geq 0 \middle| H_i \right\}.
\end{aligned}$$

Assume that $\Pr\{x_j = (-1)^{c_{\ell,j}} | H_\ell\} = 1$ for $1 \leq j \leq N$. Then, $\{(y_j|H_i)\}_{j=1}^N$ is independent Gaussian distributed with marginal mean $(-1)^{c_{i,j}}$ and common marginal variance σ^2 if $\mathbb{T}$ is a diagonal matrix with equal diagonal $\sigma = \sqrt{N_0/2}$. As a result, $\sum_{\{j \,:\, c_{\ell,j}=0, c_{i,j}=1\}} y_j - \sum_{\{j \,:\, c_{\ell,j}=1, c_{i,j}=0\}} y_j$ is Gaussian distributed with mean $-d(\boldsymbol{c}_\ell, \boldsymbol{c}_i)$ and variance $\sigma^2 \cdot d(\boldsymbol{c}_\ell, \boldsymbol{c}_i)$, and

$$\begin{aligned}
\Pr[\text{error}] &\leq \frac{1}{M} \sum_{i=0}^{M-1} \sum_{\ell=0, \ell \neq i}^{M-1} \Pr\left\{ \sum_{\{j \,:\, c_{\ell,j}=0, c_{i,j}=1\}} y_j - \sum_{\{j \,:\, c_{\ell,j}=1, c_{i,j}=0\}} y_j \geq 0 \middle| H_i \right\} \\
&= \frac{1}{M} \sum_{i=0}^{M-1} \sum_{\ell=0, \ell \neq i}^{M-1} \int_0^\infty \frac{1}{\sqrt{2\pi\sigma^2 d(\boldsymbol{c}_\ell, \boldsymbol{c}_i)}} \exp\left\{ -\frac{[y + d(\boldsymbol{c}_\ell, \boldsymbol{c}_i)]^2}{2\sigma^2 d(\boldsymbol{c}_\ell, \boldsymbol{c}_i)} \right\} dy \\
&= \frac{1}{M} \sum_{i=0}^{M-1} \sum_{\ell=0, \ell \neq i}^{M-1} Q\left(\frac{\sqrt{d(\boldsymbol{c}_\ell, \boldsymbol{c}_i)}}{\sigma} \right). \qquad (5.1)
\end{aligned}$$

We then search for the code matrix that minimizes (5.1). As criterion (5.1)

is apparently a function of the Hamming distances among codewords, it can be anticipated that a larger minimum pairwise Hamming distance will result in a smaller (5.1) quantity.

In our later computer searches, we found that the quantity σ, when it is confined with the range (equivalently, the signal-to-noise ratio range) considered in this work, does not affect the best code obtained. However, it is expected to have certain impact on the code search result when it is taken extremely small (e.g., $\sigma \approx 0$) or extremely large (e.g., $\sigma \approx \infty$), which is of secondary interest. We list the found codes for different M in the below table, which will be used in our simulations in subsequent chapters.

Table 5.1: The code matrices that minimize (5.1), which are obtained by exhaustive computer search.

H_0	0	0	0	0	0	0	0	0	0	0
H_1	0	0	0	1	1	1	1	1	1	1
H_2	1	1	1	0	0	0	1	1	1	1

H_0	0	0	0	0	0	0	0	0	0	0
H_1	0	0	0	1	1	1	1	1	1	1
H_2	1	1	1	0	0	0	0	1	1	1
H_3	1	1	1	1	1	1	1	0	0	0

H_0	0	0	0	0	0	0	0	0	0	0
H_1	0	0	0	0	1	1	1	1	1	1
H_2	0	1	1	1	0	0	0	1	1	1
H_3	1	0	1	1	0	1	1	0	0	1
H_4	1	1	0	1	1	0	1	0	1	0

Chapter 6

Simulation Results

In this chapter, we examine the performance of the minimum Euclidean distance fusion rule through simulations. According to the system model introduced in Chapter 2, a WSN system with hypothesis number M and sensor number N is simulated. We assume that all sensor observations have the same distribution given each hypothesis, and are randomly drawn from a σ^2-variance Gaussian distribution with means $m_0, m_1, \cdots, m_{M-1}$ corresponding to hypothesis $H_0, H_1, \cdots, H_{M-1}$, respectively. Also, Each sensor makes the local classification based on the thresholds $\frac{m_0+m_1}{2}, \frac{m_1+m_2}{2}, \cdots, \frac{m_{M-2}+m_{M-1}}{2}$. Accordingly, OSNR is defined as $\frac{\left[(m_1-m_0)^2+(m_2-m_1)^2+\cdots+(m_{M-1}-m_{M-2})^2\right]/(M-1)}{\sigma^2}$, while CSNR is given by $\frac{1}{2\cdot \mathrm{tr}(\mathbb{C})/N}$, where $\mathbb{C}$ is the channel covariance matrix.

In subsequent sections, we will provide simulation results for three different link noise models. Under each link noise model, three code matrices as listed in Tab. 5.1 are simulated. The faulty sensors are uniformly drawn from the N deployed sensor nodes. As revealed by their names, the faulty sensor always send one regardless of the local measurements when stuck-at-one fault is considered. Similarly, stuck-at-zero fault sensors always transmit

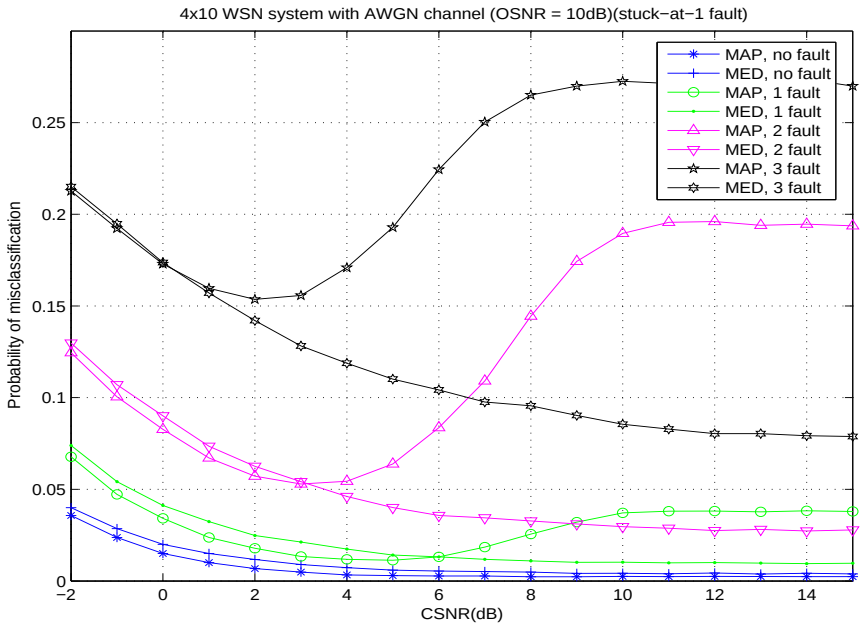

Figure 6.1: Performance of the MAP rule and the MED rule under AWGN channel at OSNR=10 dB for stuck-at-1 faults when 4×10 code matrix is employed.

zero to the fusion center. When random fault occurs, the faulty sensors send one and zero with equal probability.

6.1 AWGN wireless noise links

Under AWGN wireless noise links, the MAP fusion rule specified in (3.1) and the minimum Euclidean distance (MED) fusion rule specified in (3.2) are implemented in our simulations. From Figs. 6.1 and 6.2, we observe that the MAP fusion rule has better performance than the MED fusion rule at fault-free situation as anticipated. However, when sensor faults occur, the

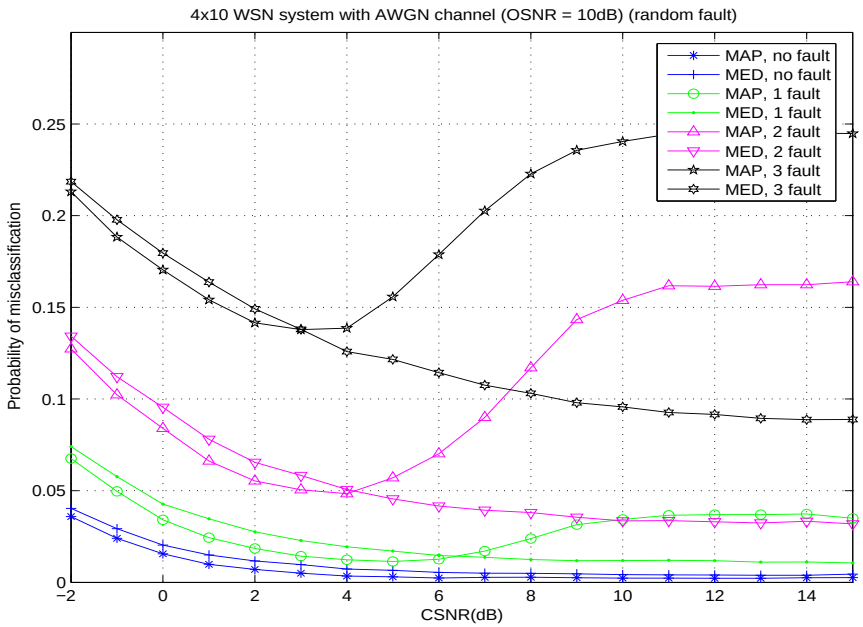

Figure 6.2: Performance of the MAP rule and the MED rule under AWGN channel at OSNR=10 dB for random faults when 4×10 code matrix is employed.

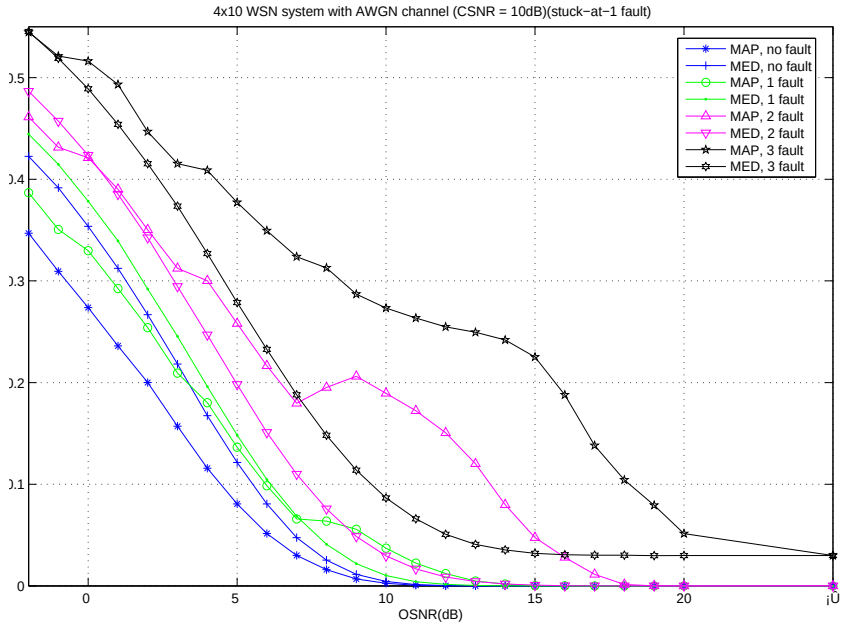

Figure 6.3: Performance of the MAP rule and the MED rule under AWGN channel at CSNR=10 dB for stuck-at-1 faults when 4×10 code matrix is employed.

misclassification probability of the MAP fusion rule even rises up at high CSNRs because it presumably trusts all sensor outputs among which some of them are faulty. As a contrary, the performance of the MED fusion rule remains decreasing with respect to CSNR, and is more robust to sensor faults than the MAP fusion rule.

The robustness of the MED fusion against sensor faults can also be observed in Figs. 6.3 and 6.4, where OSNR is used as an argument instead of CSNR. Again, when sensor faults occur, the performance of the MAP fusion rule becomes worse than the MED fusion rule at high OSNRs. Further, as

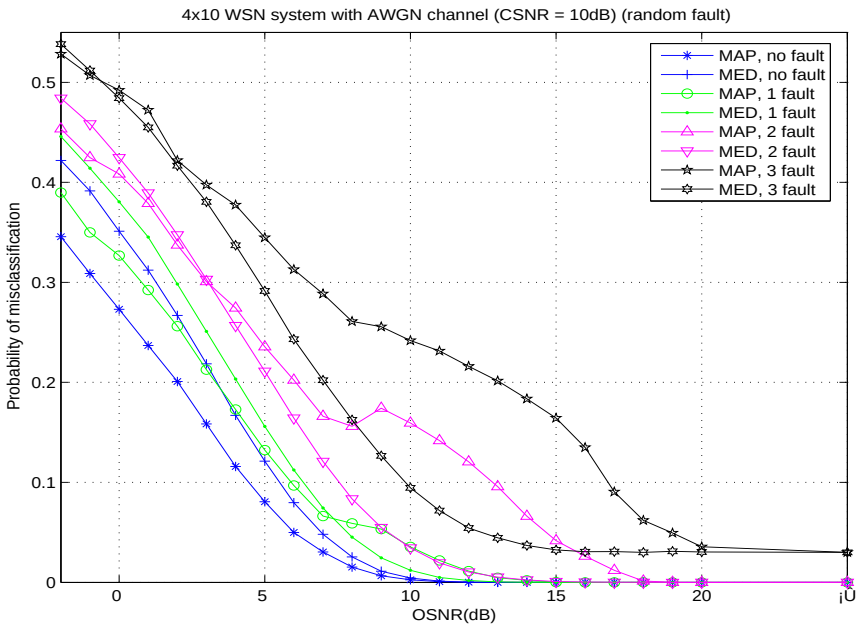

Figure 6.4: Performance of the MAP rule and the MED rule under AWGN channel at CSNR=10 dB for random faults when 4×10 code matrix is employed.

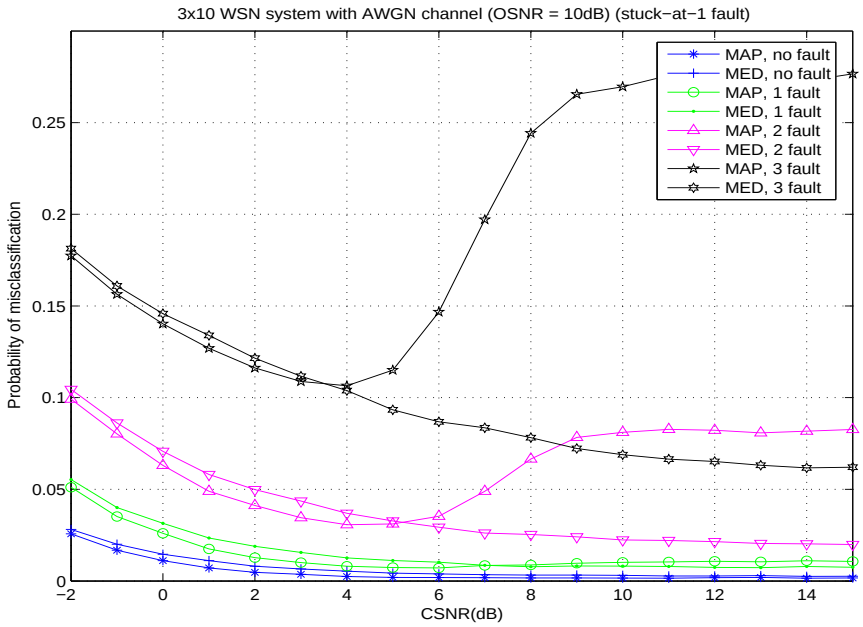

Figure 6.5: Performance of the MAP rule and the MED rule under AWGN channel at OSNR=10 dB for stuck-at-1 faults when 3×10 code matrix is employed.

mentioned in Section 3.2, in a fault-free situation, the MED fusion rule performs close to the MAP fusion rule when the local classification is sufficiently accurate.

Repeating the above simulations with 3×10 and 5×10 code matrices in Tab. 5.1 yields similar conclusions, where the results are displayed in Figs. 6.5–6.12.

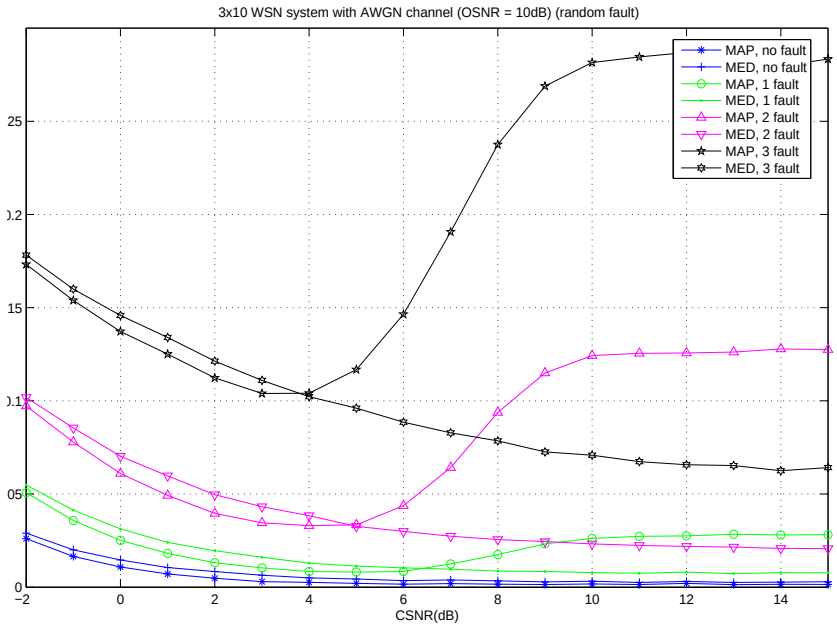

Figure 6.6: Performance of the MAP rule and the MED rule under AWGN channel at OSNR=10 dB for random faults when 3×10 code matrix is employed.

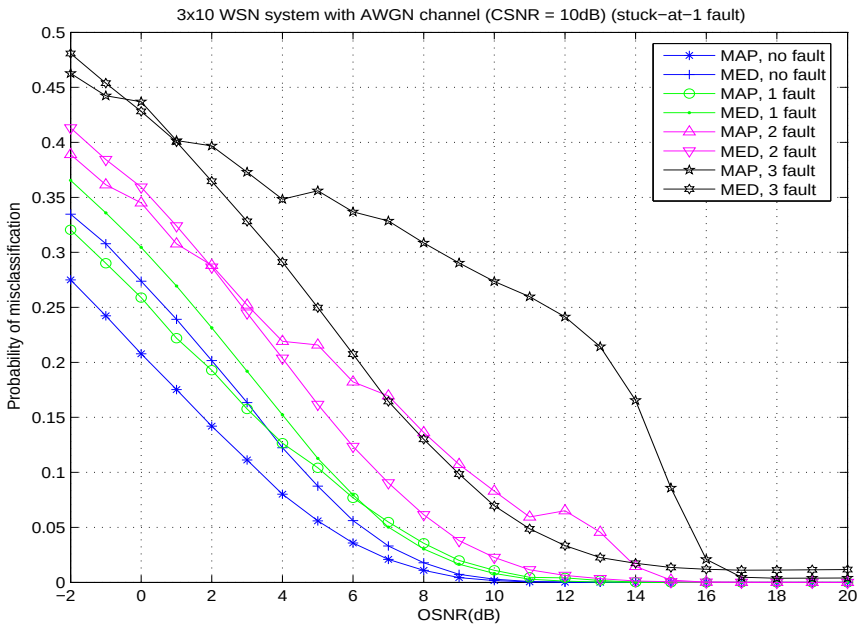

Figure 6.7: Performance of the MAP rule and the MED rule under AWGN channel at CSNR=10 dB for stuck-at-1 faults when 3×10 code matrix is employed.

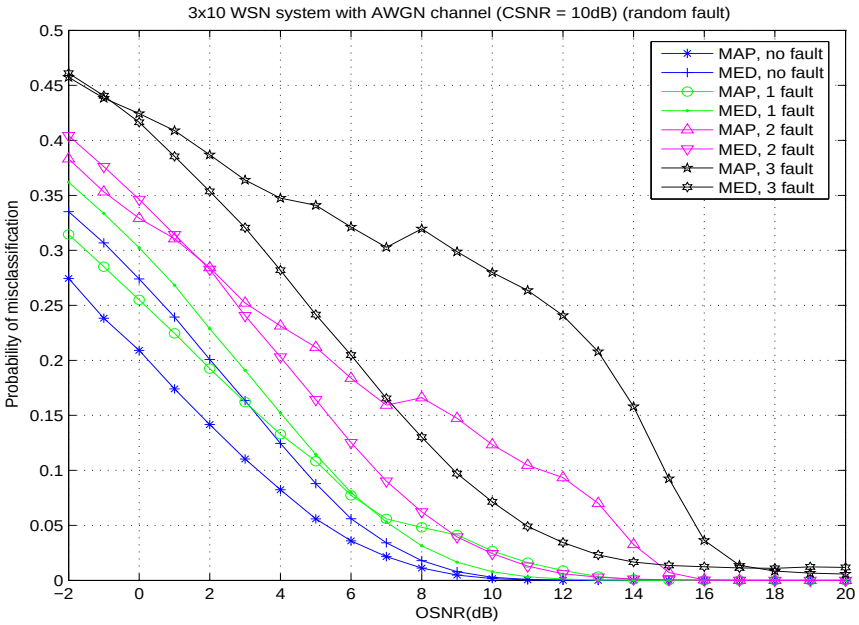

Figure 6.8: Performance of the MAP rule and the MED rule under AWGN channel at CSNR=10 dB for random faults when 3×10 code matrix is employed.

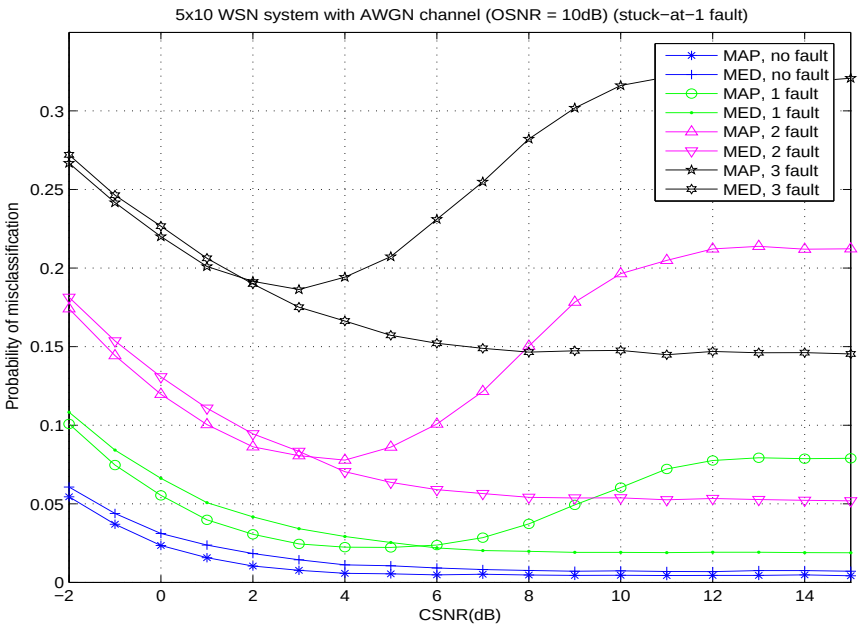

Figure 6.9: Performance of the MAP rule and the MED rule under AWGN channel at OSNR=10 dB for stuck-at-1 faults when 5×10 code matrix is employed.

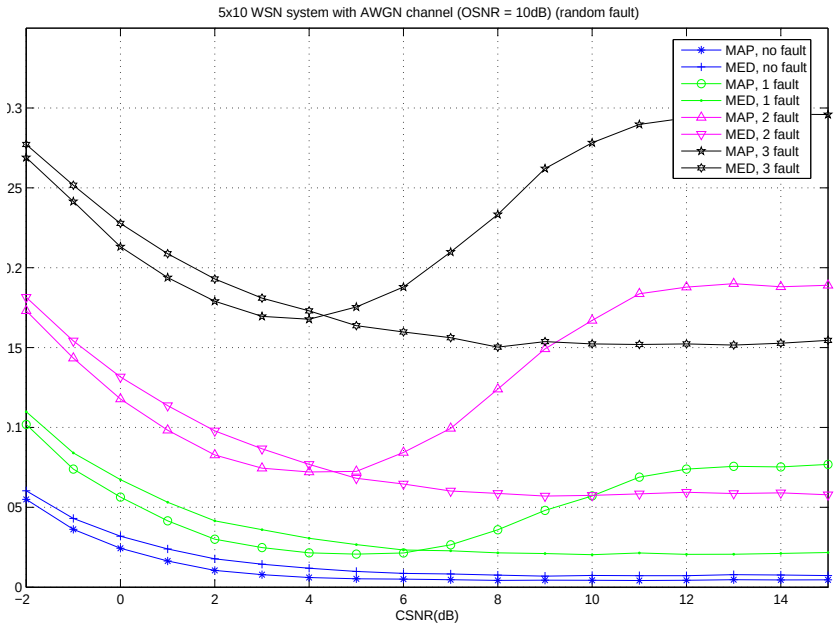

Figure 6.10: Performance of the MAP rule and the MED rule under AWGN channel at OSNR=10 dB for random faults when 5×10 code matrix is employed.

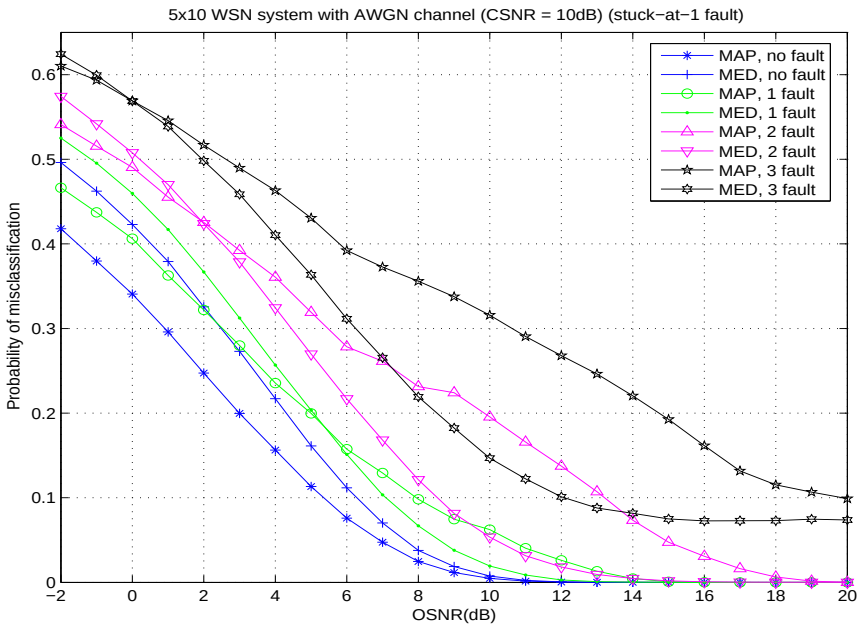

Figure 6.11: Performance of the MAP rule and the MED rule under AWGN channel at CSNR=10 dB for stuck-at-1 faults when 5×10 code matrix is employed.

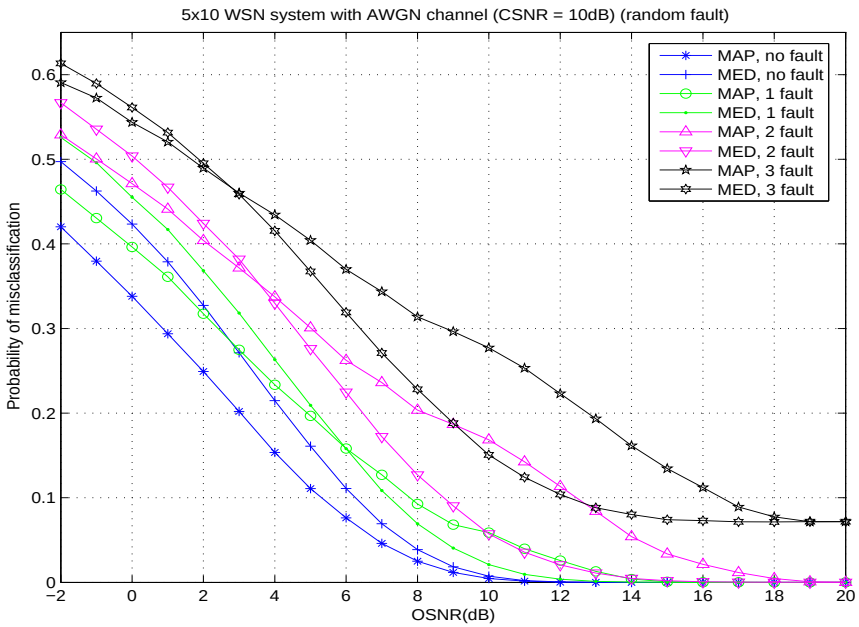

Figure 6.12: Performance of the MAP rule and the MED rule under AWGN channel at CSNR=10 dB for random faults when 5×10 code matrix is employed.

6.2 Spatially correlated wireless link noises

Within a WSN, the information from sensors is often gathered inside a small area. Thus, the adjacent link noises may be correlated with each other. Hence, in this section, spatially correlated wireless link noises are considered instead of the AWGN, where the channel covariance matrix is devised of the form:

$$\mathbb{C} = \sigma^2 \begin{bmatrix} 1 & \rho & \rho & \cdots & \rho \\ \rho & 1 & \rho & \cdots & \rho \\ \rho & \rho & 1 & \cdots & \rho \\ \vdots & \vdots & \vdots & \ddots & \vdots \\ \rho & \rho & \rho & \cdots & 1 \end{bmatrix}.$$

With the help of the training sequence, channel estimation and equalization at the fusion becomes possible. By adopting the ML estimator in (4.1), our results show that the longer the training sequence, the better the system performance. When there are several faulty sensors, the system performance with training becomes even better than the system performance with known covariance matrix, since the training procedure also helps the fusion adapt the sensor fault situation. Specifically, it can be seen from Figs. 6.13–6.16, the misclassification probability decreases as the number of training vectors increases from 15 to 35.

Similar observations can be made from Figs. 6.17–6.20 with different

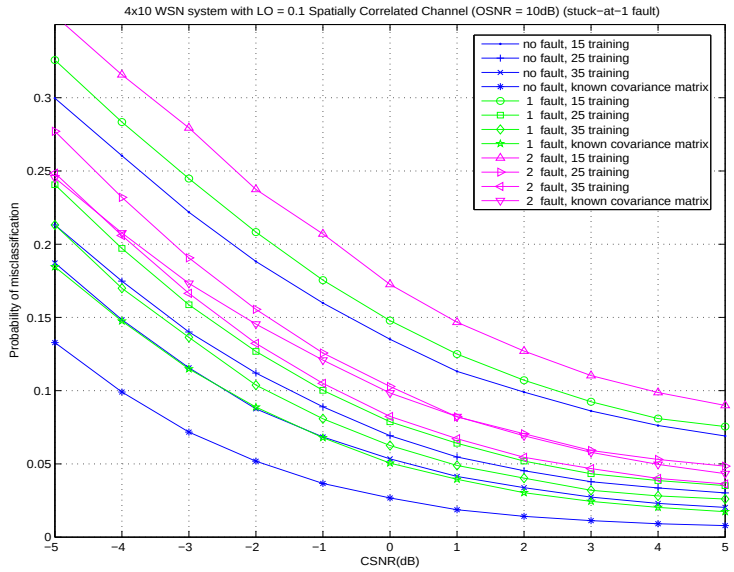

Figure 6.13: Performance of the MED rule under $\rho = 0.1$ spatially correlated channel at OSNR=10 dB for stuck-at-1 faults when 4×10 code matrix is employed.

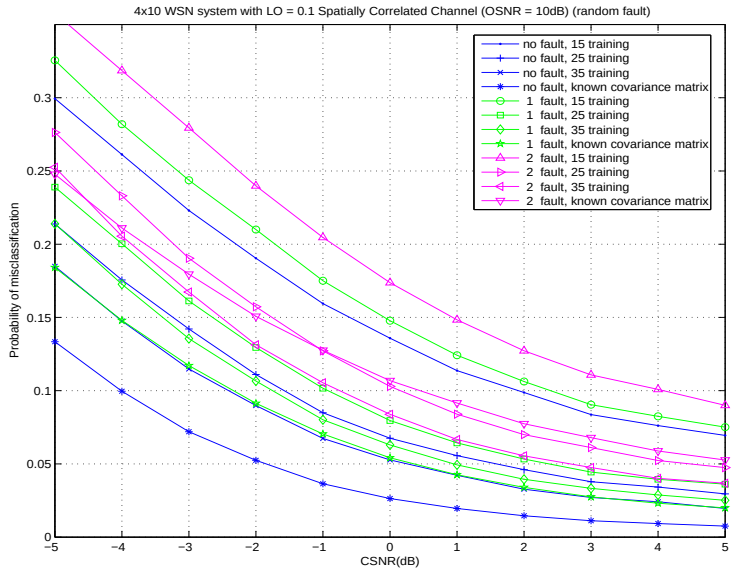

Figure 6.14: Performance of the MED rule under $\rho = 0.1$ spatially correlated channel at OSNR=10 dB for random faults when 4×10 code matrix is employed.

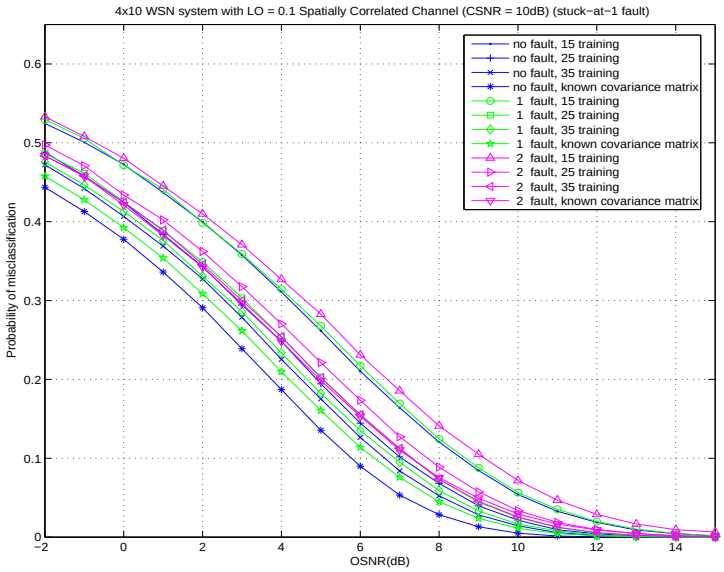

Figure 6.15: Performance of the MED rule under $\rho = 0.1$ spatially correlated channel at CSNR=10 dB for stuck-at-1 faults when 4×10 code matrix is employed.

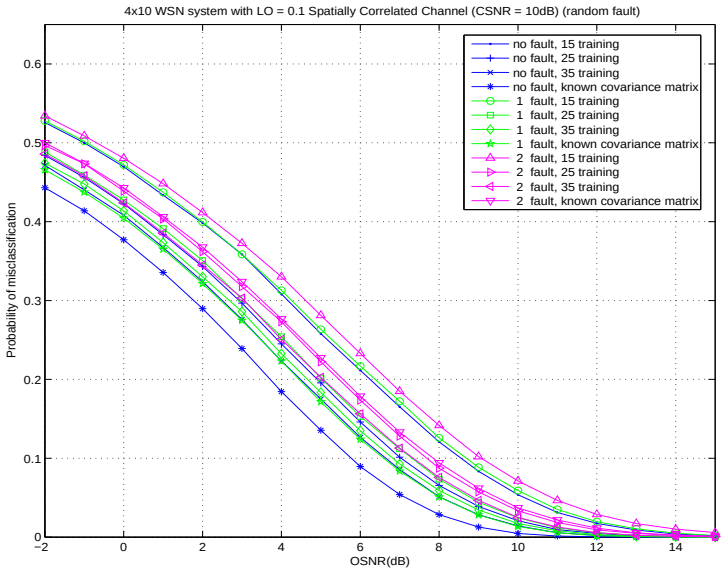

Figure 6.16: Performance of the MED rule under $\rho = 0.1$ spatially correlated channel at CSNR=10 dB for random faults when 4×10 code matrix is employed.

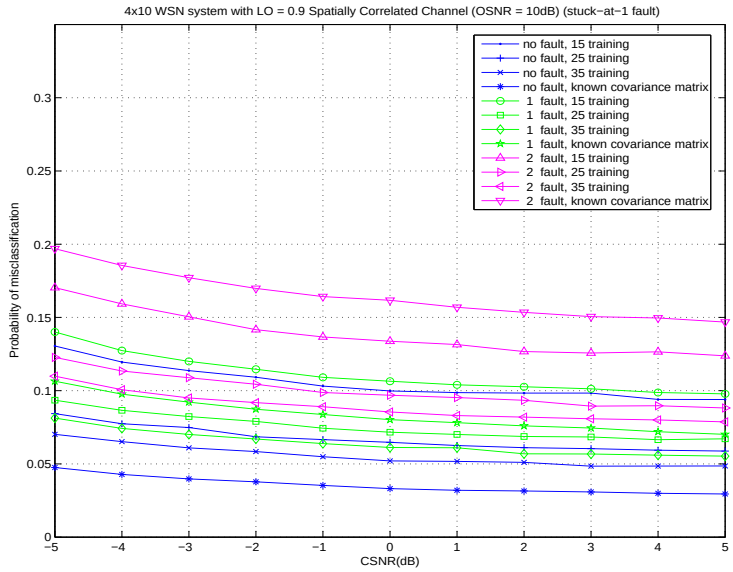

Figure 6.17: Performance of the MED rule under $\rho = 0.9$ spatially correlated channel at OSNR=10 dB for stuck-at-1 faults when 4×10 code matrix is employed.

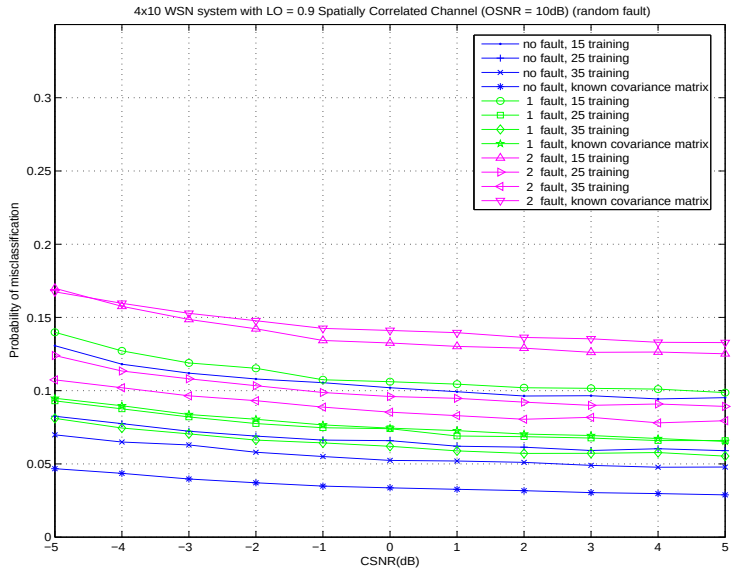

Figure 6.18: Performance of the MED rule under $\rho = 0.9$ spatially correlated channel at OSNR=10 dB for random faults when 4×10 code matrix is employed.

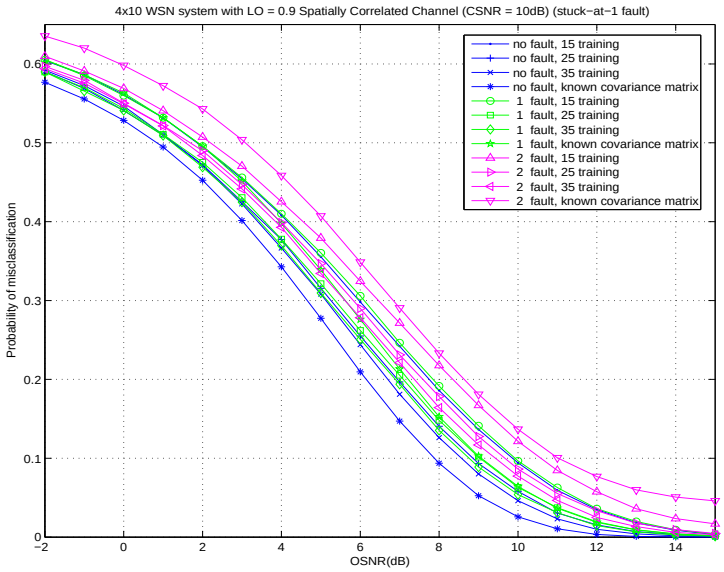

Figure 6.19: Performance of the MED rule under $\rho = 0.9$ spatially correlated channel at CSNR=10 dB for stuck-at-1 faults when 4×10 code matrix is employed.

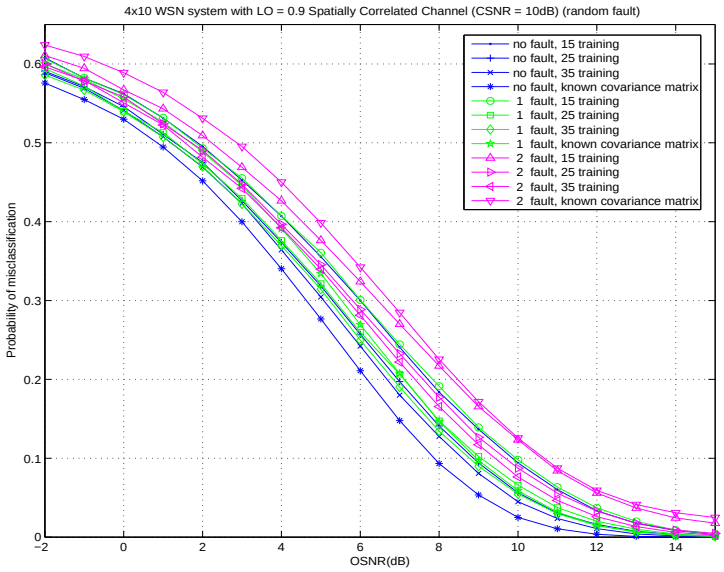

Figure 6.20: Performance of the MED rule under $\rho = 0.9$ spatially correlated channel at CSNR=10 dB for random faults when 4×10 code matrix is employed.

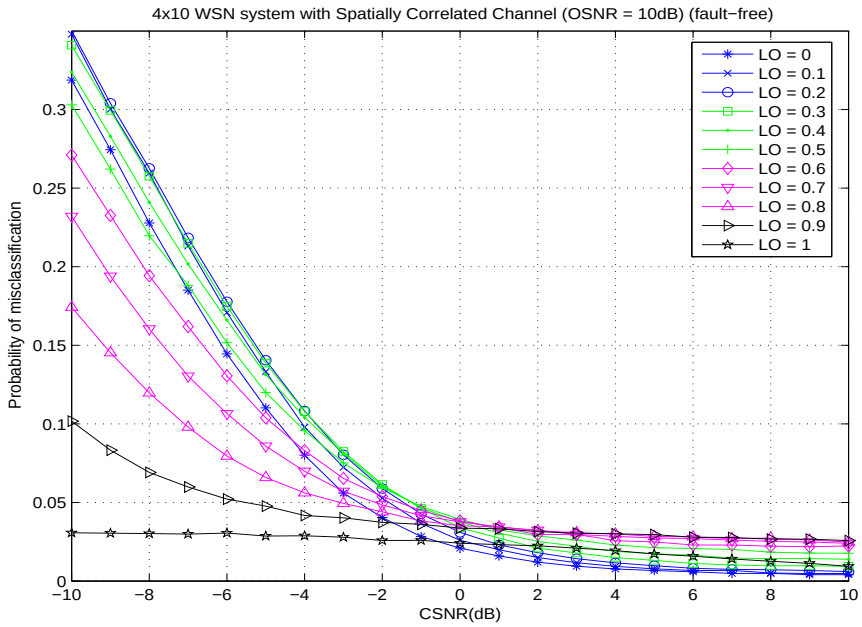

Figure 6.21: Performance of the MED rule with perfect channel estimation under spatially correlated channel at OSNR=10 dB in fault-free situation when 4×10 code matrix is employed.

correlation coefficient $\rho = 0.9$.

Comparing Fig. 6.13 with Fig. 6.17, we can see that the performances curves corresponding to different channel correlation are distinct. We summarize in Figs. 6.21 and 6.22 the system performances corresponding to different correlation factors under perfect channel estimation.

In Fig. 6.21, we observe that the performance curve turns flatter as ρ grows. Thus, when channel correlation increases, the system performance becomes irrelevant to the CSNR. This phenomenon can be explained through the extreme case of $\rho = 1$, in which case the channel link noises are all

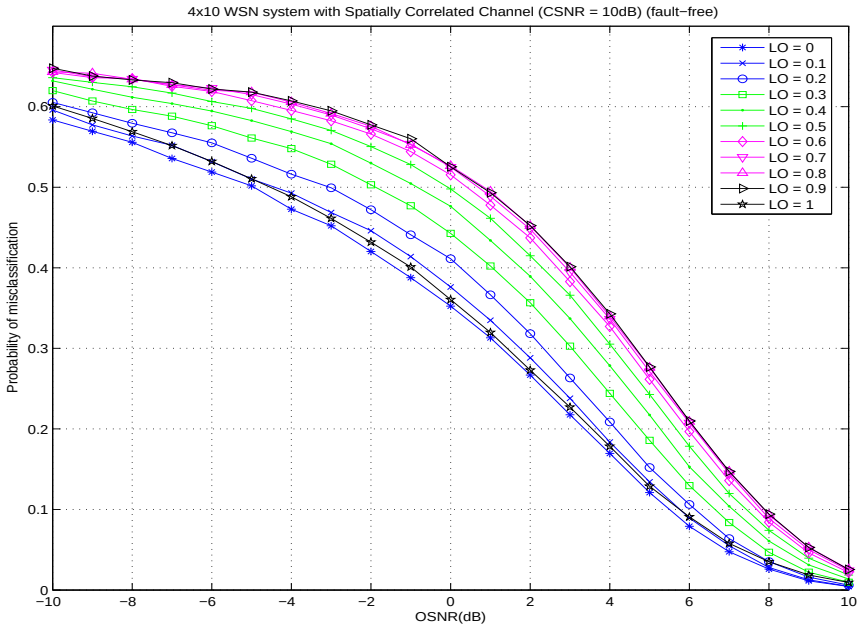

Figure 6.22: Performance of the MED rule with perfect channel estimation under spatially correlated channel at CSNR=10 dB in fault-free situation when 4×10 code matrix is employed.

equal. Then, no matter how small the CSNR is, the fusion center can easily identify the noise quantity by receiving multiple sensor signals; hence, the performance has no improvement by increasing the CSNR.

In addition, there are two distinct behaviors in the relationship between channel correlation ρ and system performance. At low CSNR, the system performance improves as ρ increases, while at high CSNR, the system performance is worse for smaller ρ. The former case can be justified by the same reason stated in the previous paragraph. A possible reason for the latter case is that the DCFECC code matrix adopted here is searched under the uncorrelated channel assumption, namely, $\rho = 0$, and the same code may not be optimal when a non-zero ρ is considered. Similar trends on how the system performance varies with ρ can be observed in Fig. 6.22.

Repeating the above simulations with 3×10 and 5×10 code matrices under $\rho = 0.1$ and 0.9 yields Figs. 6.23–6.38, from which the same conclusion can be drawn.

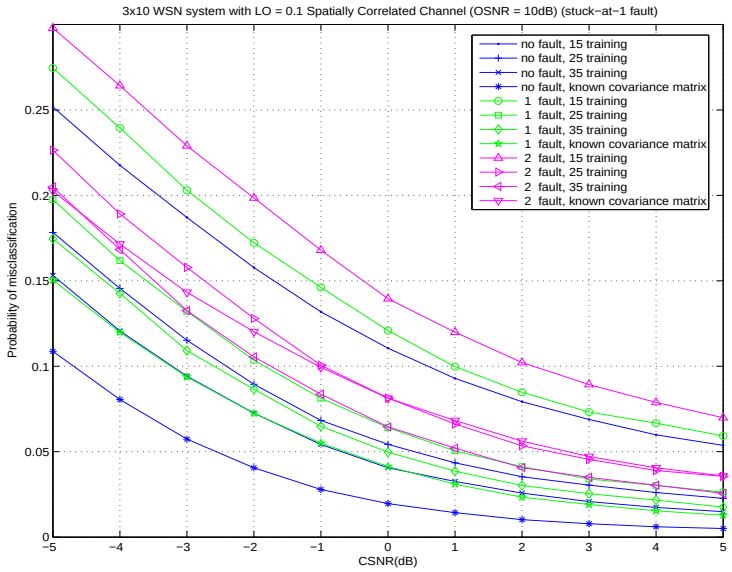

Figure 6.23: Performance of the MED rule under $\rho = 0.1$ spatially correlated channel at OSNR=10 dB for stuck-at-1 faults when 3×10 code matrix is employed.

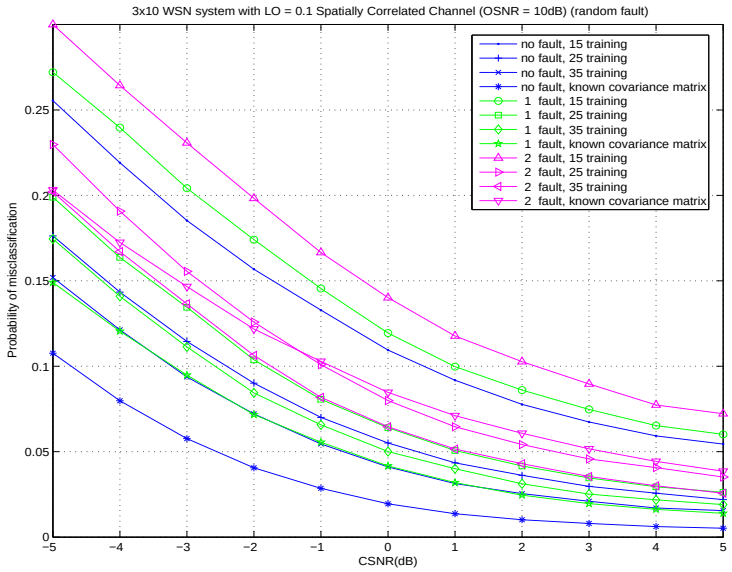

Figure 6.24: Performance of the MED rule under $\rho = 0.1$ spatially correlated channel at OSNR=10 dB for random faults when 3×10 code matrix is employed.

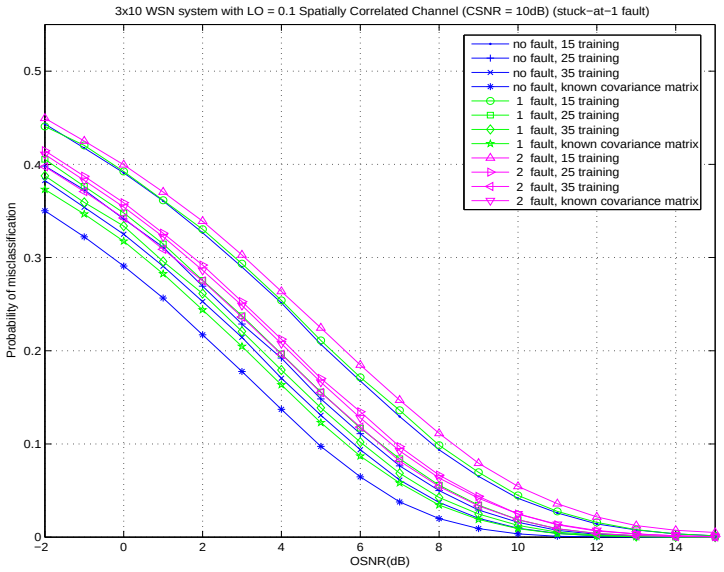

Figure 6.25: Performance of the MED rule under $\rho = 0.1$ spatially correlated channel at CSNR=10 dB for stuck-at-1 faults when 3×10 code matrix is employed.

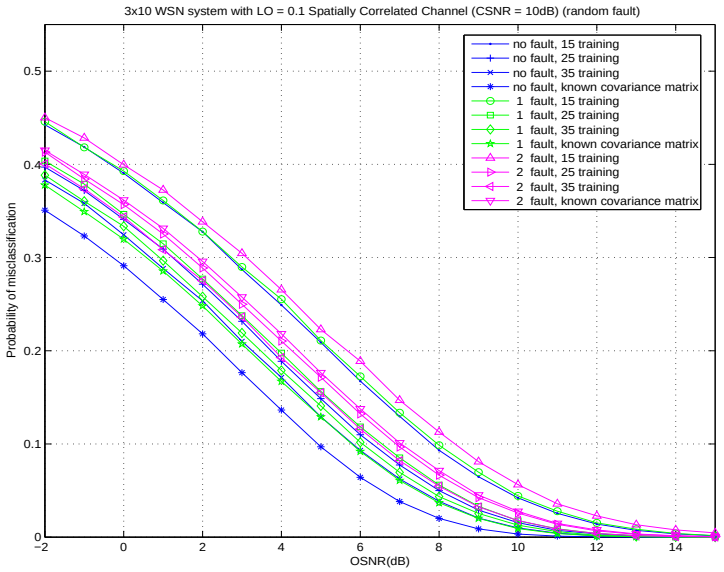

Figure 6.26: Performance of the MED rule under $\rho = 0.1$ spatially correlated channel at CSNR=10 dB for random faults when 3×10 code matrix is employed.

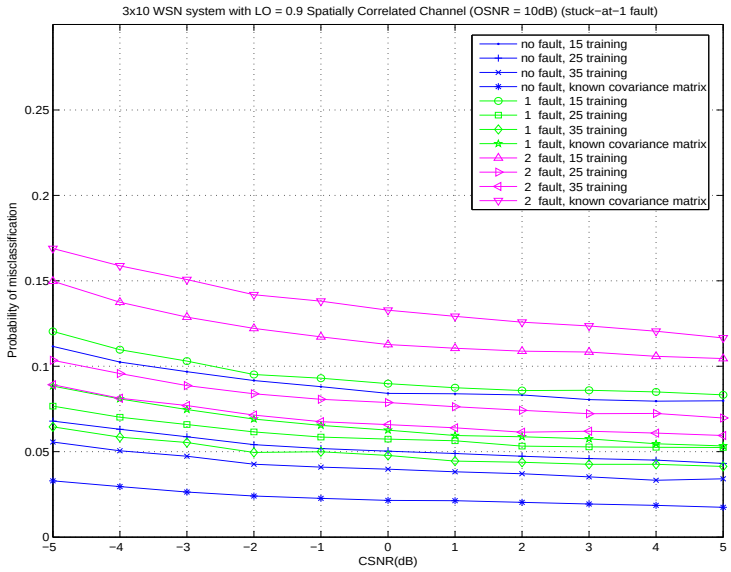

Figure 6.27: Performance of the MED rule under $\rho = 0.9$ spatially correlated channel at OSNR=10 dB for stuck-at-1 faults when 3×10 code matrix is employed.

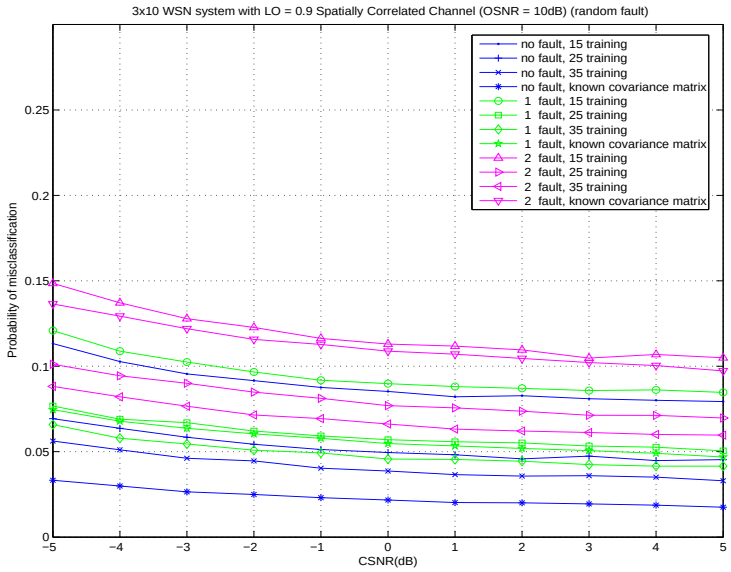

Figure 6.28: Performance of the MED rule under $\rho = 0.9$ spatially correlated channel at OSNR=10 dB for random faults when 3×10 code matrix is employed.

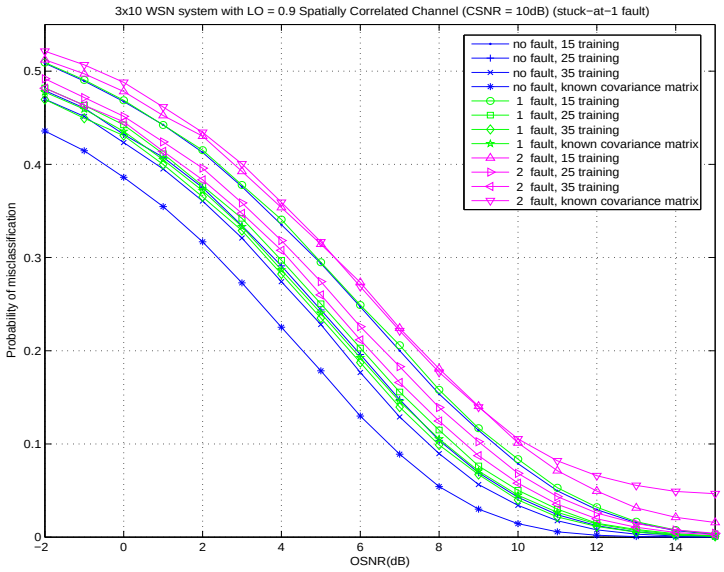

Figure 6.29: Performance of the MED rule under $\rho = 0.9$ spatially correlated channel at CSNR=10 dB for stuck-at-1 faults when 3×10 code matrix is employed.

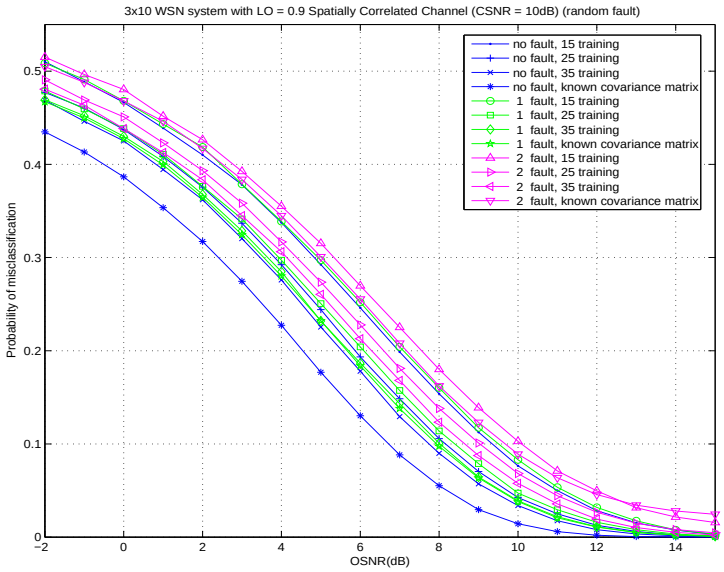

Figure 6.30: Performance of the MED rule under $\rho = 0.9$ spatially correlated channel at CSNR=10 dB for random faults when 3×10 code matrix is employed.

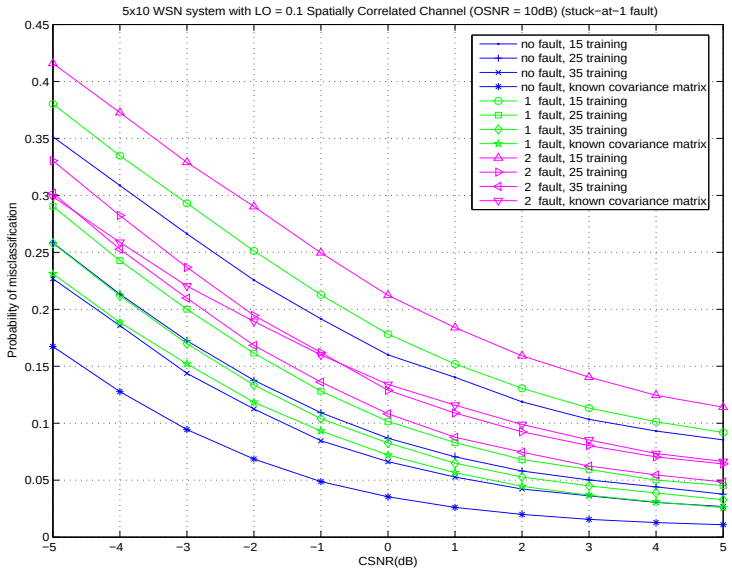

Figure 6.31: Performance of the MED rule under $\rho = 0.1$ spatially correlated channel at OSNR=10 dB for stuck-at-1 faults when 5×10 code matrix is employed.

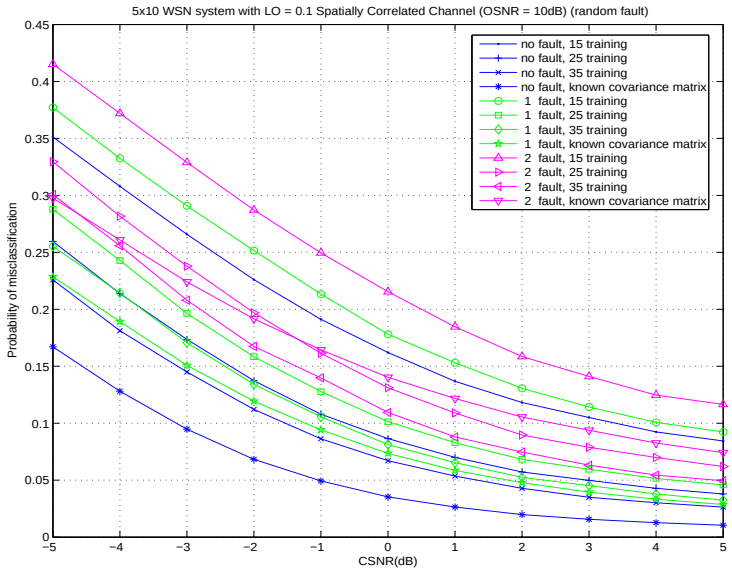

Figure 6.32: Performance of the MED rule under $\rho = 0.1$ spatially correlated channel at OSNR=10 dB for random faults when 5×10 code matrix is employed.

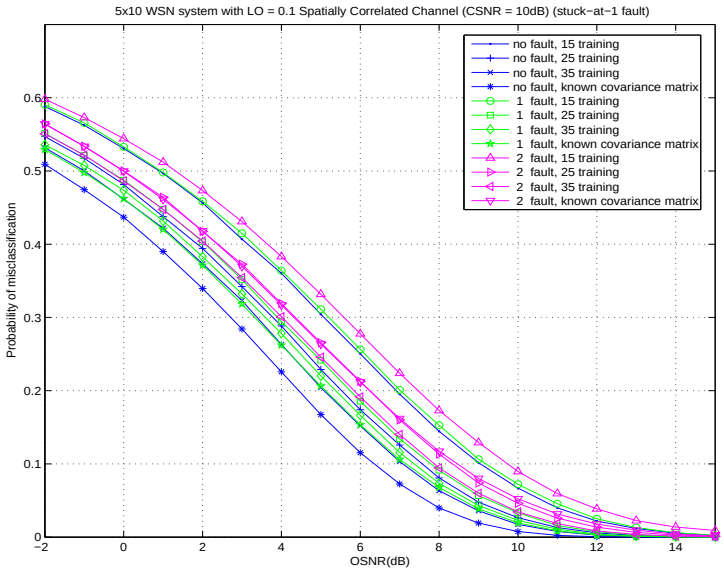

Figure 6.33: Performance of the MED rule under $\rho = 0.1$ spatially correlated channel at CSNR=10 dB for stuck-at-1 faults when 5×10 code matrix is employed.

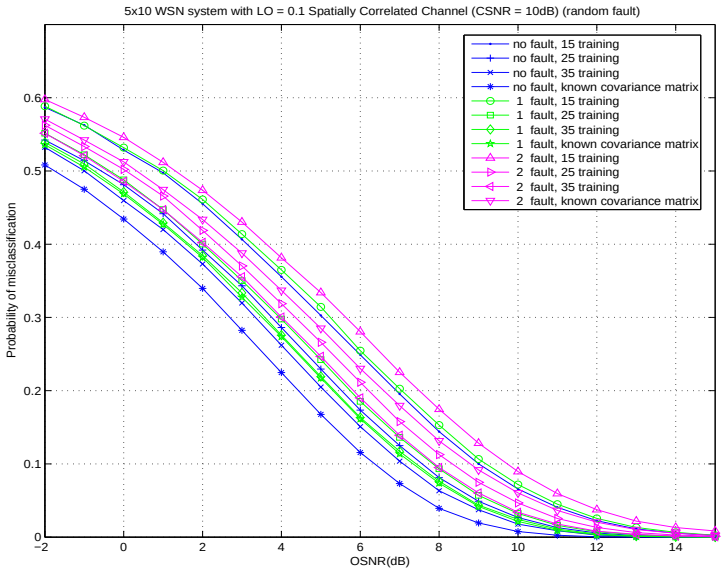

Figure 6.34: Performance of the MED rule under $\rho = 0.1$ spatially correlated channel at CSNR=10 dB for random faults when 5×10 code matrix is employed.

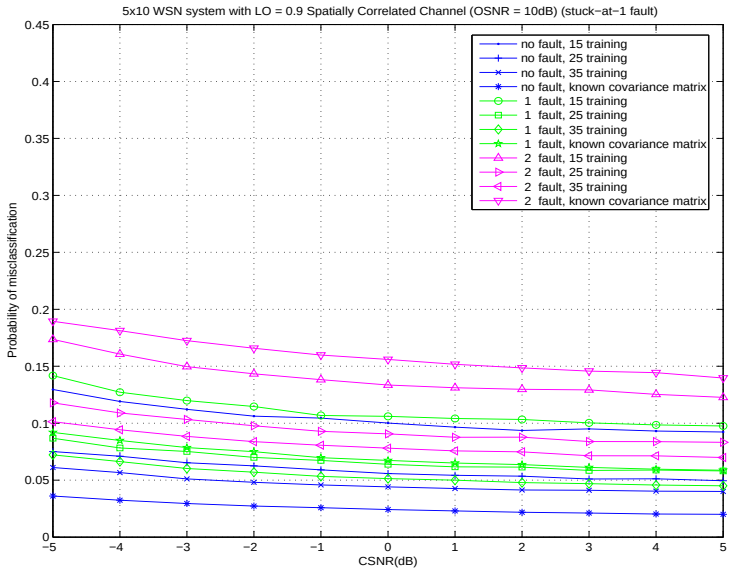

Figure 6.35: Performance of the MED rule under $\rho = 0.9$ spatially correlated channel at OSNR=10 dB for stuck-at-1 faults when 5×10 code matrix is employed.

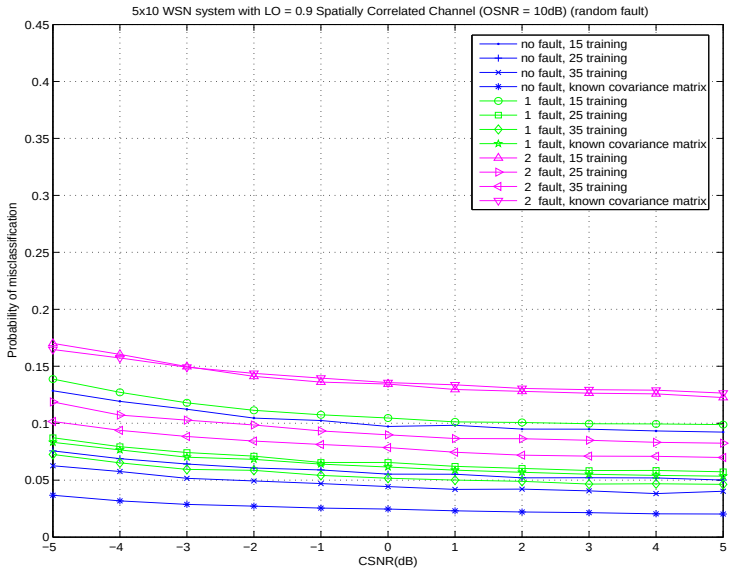

Figure 6.36: Performance of the MED rule under $\rho = 0.9$ spatially correlated channel at OSNR=10 dB for random faults when 5×10 code matrix is employed.

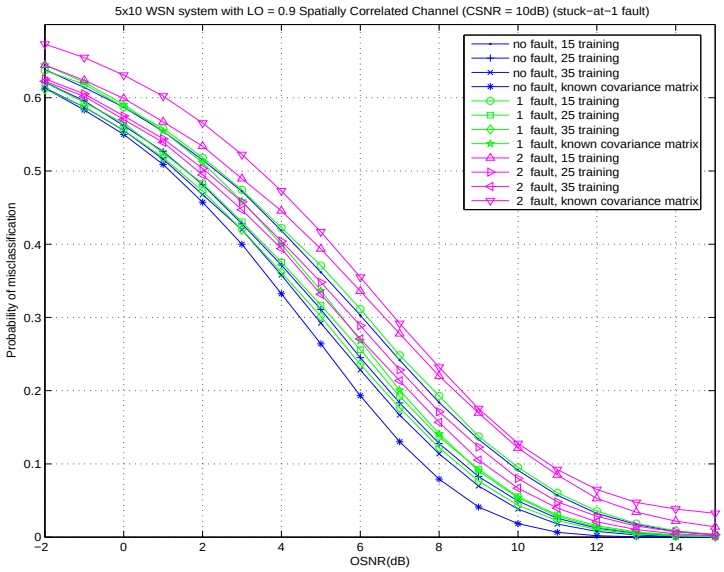

Figure 6.37: Performance of the MED rule under $\rho = 0.9$ spatially correlated channel at CSNR=10 dB for stuck-at-1 faults when 5×10 code matrix is employed.

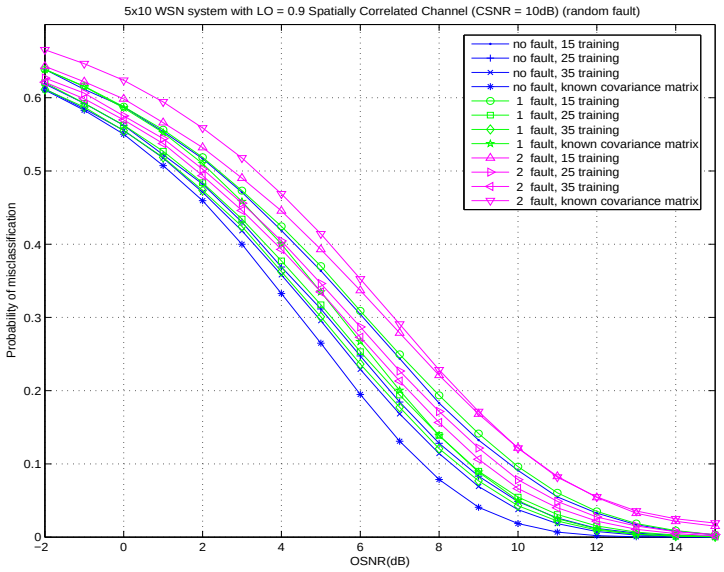

Figure 6.38: Performance of the MED rule under $\rho = 0.9$ spatially correlated channel at CSNR=10 dB for random faults when 5×10 code matrix is employed.

6.3 Non-identical uncorrelated wireless link noises

In this section, we simulate the situation that the distributed sensors may have different distances to the fusion center, which results in non-identical variances in local link noises. As a simplification of the considered situation, the channel covariance matrix is devised of the form:

$$\mathbb{C} = \sigma^2 \begin{bmatrix} 1 & 0 & 0 & 0 & 0 & 0 & 0 & 0 & 0 & 0 \\ 0 & 1 & 0 & 0 & 0 & 0 & 0 & 0 & 0 & 0 \\ 0 & 0 & 1 & 0 & 0 & 0 & 0 & 0 & 0 & 0 \\ 0 & 0 & 0 & 1 & 0 & 0 & 0 & 0 & 0 & 0 \\ 0 & 0 & 0 & 0 & 1 & 0 & 0 & 0 & 0 & 0 \\ 0 & 0 & 0 & 0 & 0 & \rho & 0 & 0 & 0 & 0 \\ 0 & 0 & 0 & 0 & 0 & 0 & \rho & 0 & 0 & 0 \\ 0 & 0 & 0 & 0 & 0 & 0 & 0 & \rho & 0 & 0 \\ 0 & 0 & 0 & 0 & 0 & 0 & 0 & 0 & \rho & 0 \\ 0 & 0 & 0 & 0 & 0 & 0 & 0 & 0 & 0 & \rho \end{bmatrix}.$$

Figures 6.39–6.46 present the simulation results of 4×10 system under $\rho = 0.1$ and $\rho = 0.9$. In these figures, the effect of the ML channel estimator used in the preceding section is again illustrated.

In this section, the factor ρ becomes the deviation between two blocks of sensor link noises. To be specific, when ρ is close to one, the system returns

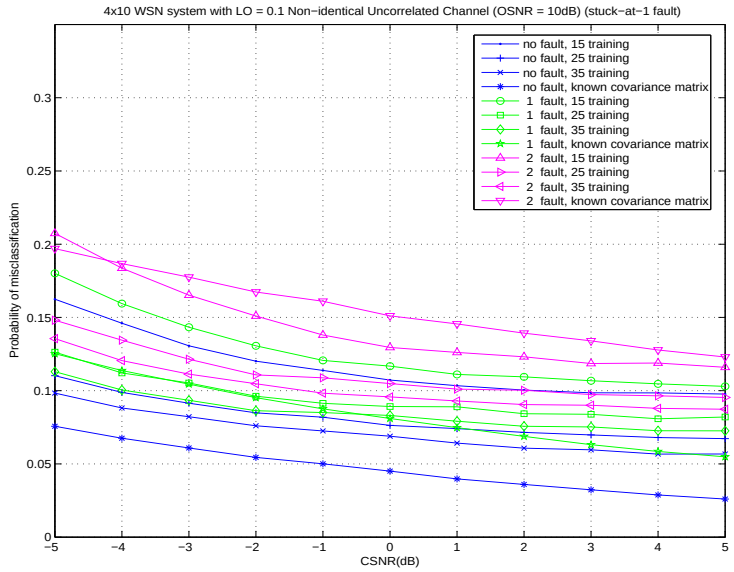

Figure 6.39: Performance of the MED rule under $\rho = 0.1$ non-identical uncorrelated channel at OSNR=10 dB for stuck-at-1 faults when 4×10 code matrix is employed.

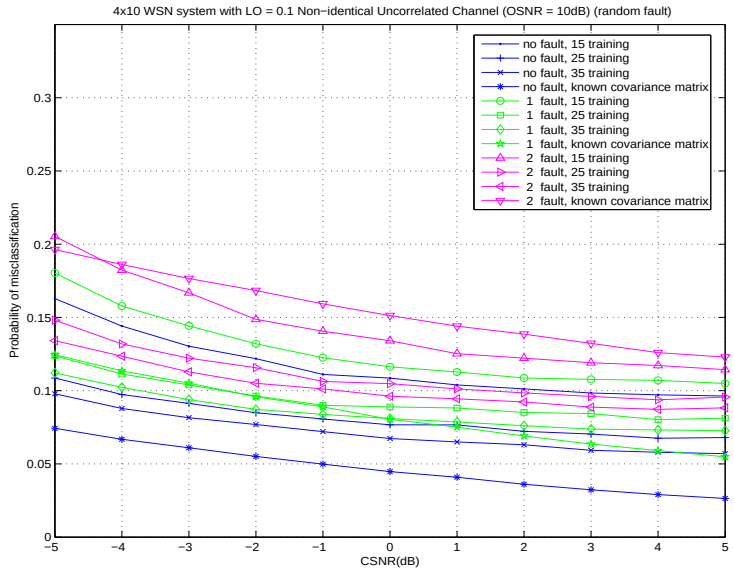

Figure 6.40: Performance of the MED rule under $\rho = 0.1$ non-identical uncorrelated channel at OSNR=10 dB for random faults when 4×10 code matrix is employed.

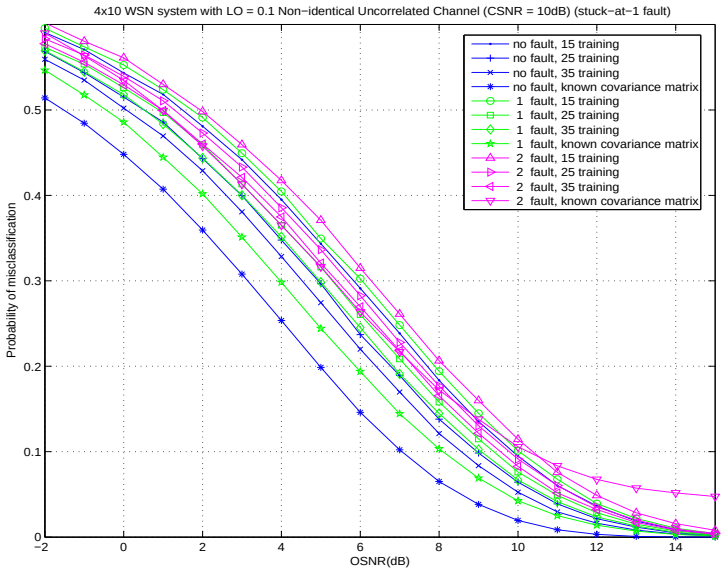

Figure 6.41: Performance of the MED rule under $\rho = 0.1$ non-identical uncorrelated channel at CSNR=10 dB for stuck-at-1 faults when 4×10 code matrix is employed.

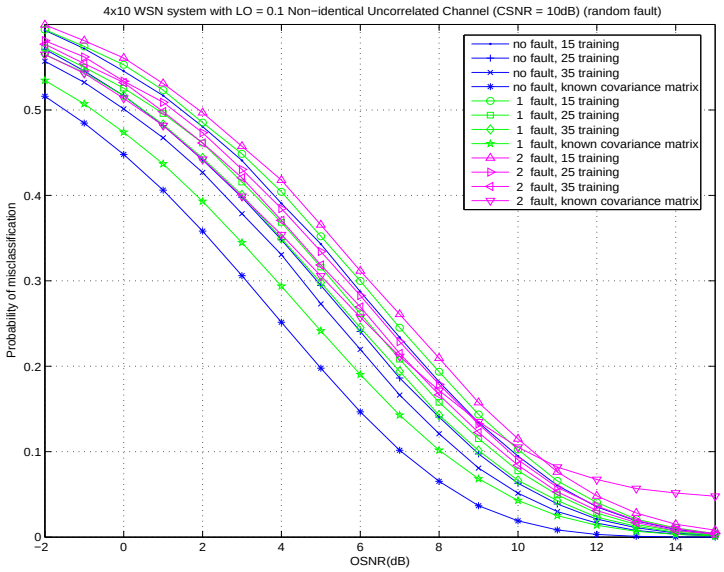

Figure 6.42: Performance of the MED rule under $\rho = 0.1$ non-identical uncorrelated channel at CSNR=10 dB for random faults when 4×10 code matrix is employed.

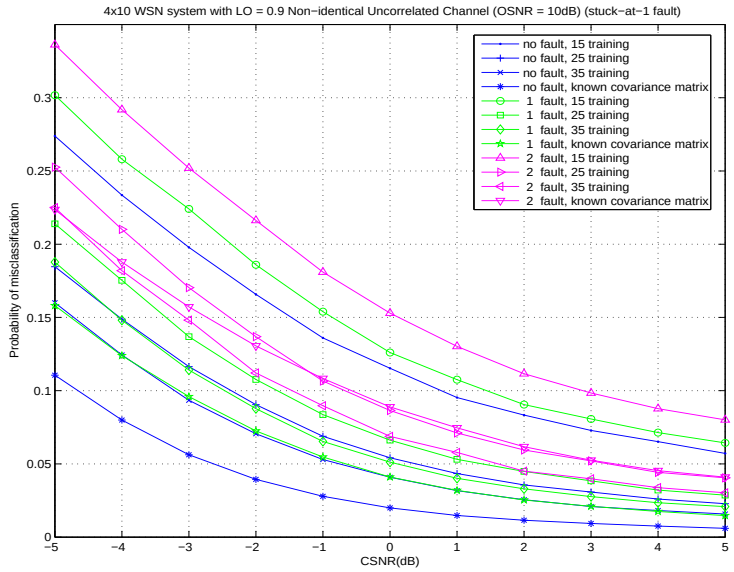

Figure 6.43: Performance of the MED rule under $\rho = 0.9$ non-identical uncorrelated channel at OSNR=10 dB for stuck-at-1 faults when 4×10 code matrix is employed.

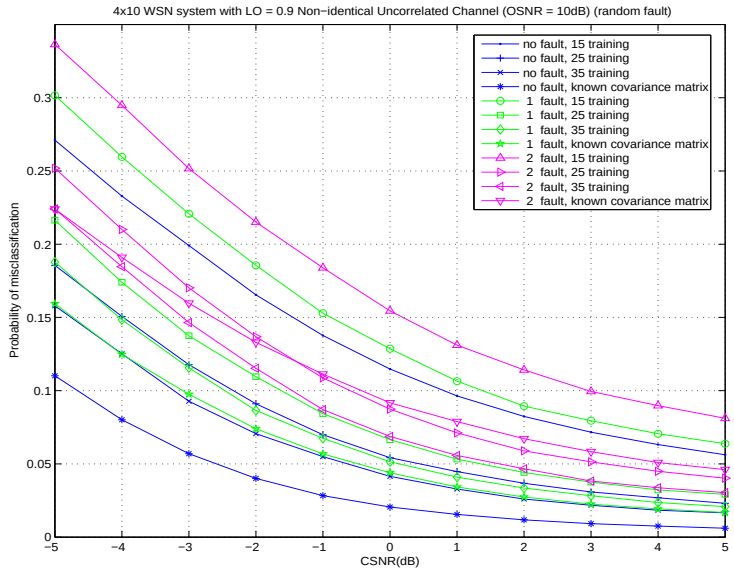

Figure 6.44: Performance of the MED rule under $\rho = 0.9$ non-identical uncorrelated channel at OSNR=10 dB for random faults when 4×10 code matrix is employed.

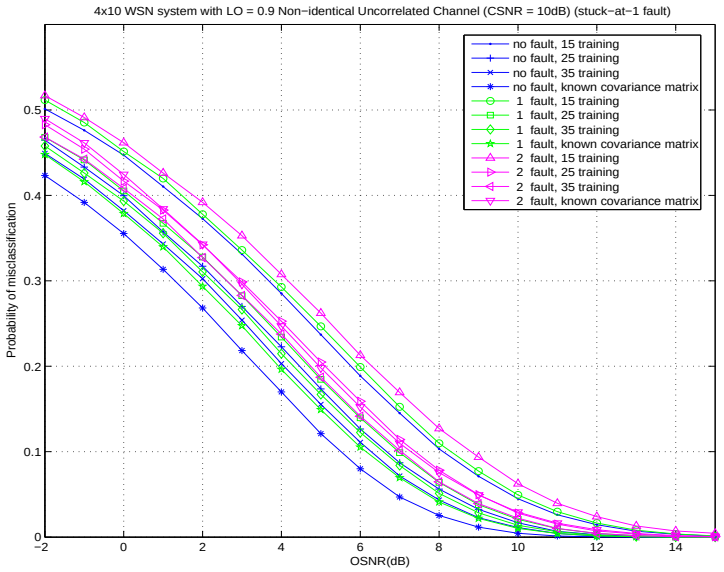

Figure 6.45: Performance of the MED rule under $\rho = 0.9$ non-identical uncorrelated channel at CSNR=10 dB for stuck-at-1 faults when 4×10 code matrix is employed.

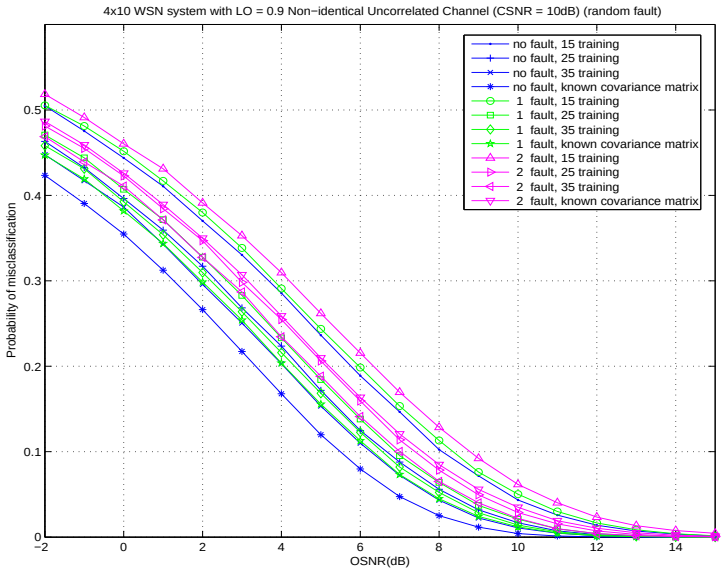

Figure 6.46: Performance of the MED rule under $\rho = 0.9$ non-identical uncorrelated channel at CSNR=10 dB for random faults when 4×10 code matrix is employed.

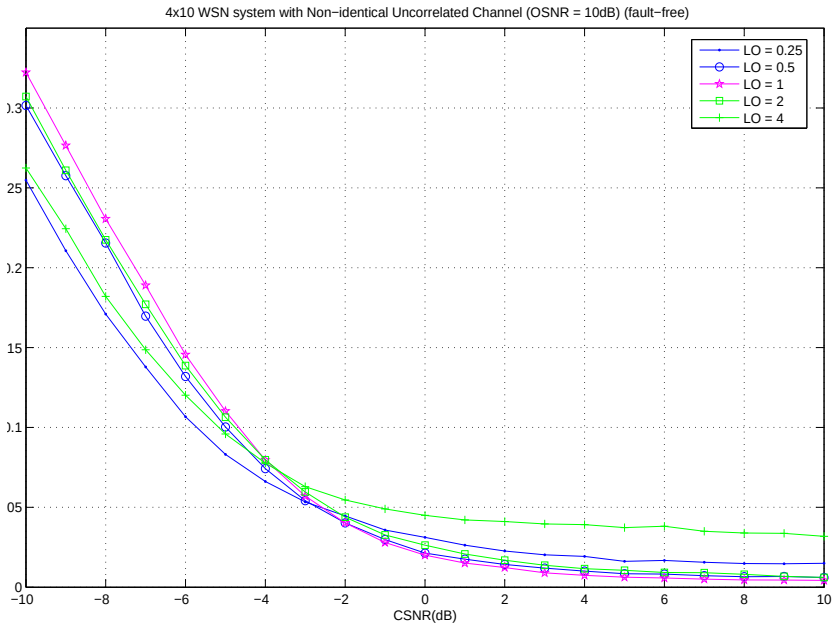

Figure 6.47: Performance of the MED rule with perfect channel estimation under non-identical uncorrelated channel at OSNR=10 dB in fault-free situation when 4×10 code matrix is employed.

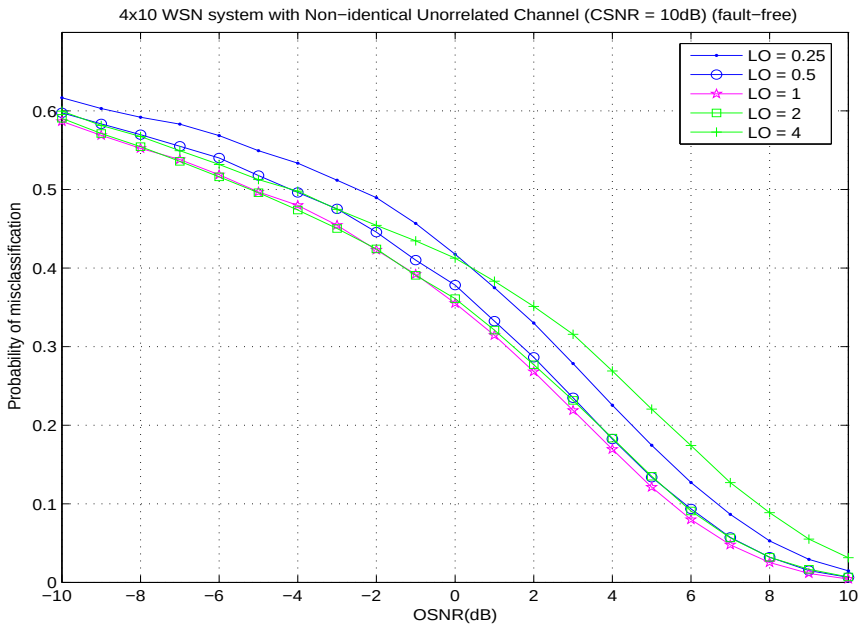

Figure 6.48: Performance of the MED rule with perfect channel estimation under non-identical uncorrelated channel at CSNR=10 dB in fault-free situation when 4×10 code matrix is employed.

to the AWGN wireless link noises. When ρ is deviated from one, five-out-of-ten sensors will have relatively low CSNR as contrary to the remaining five sensors. Figures 6.47 and 6.48 summarize the simulations.

From Fig. 6.47, we observe that the deviation between link noises can improve the performance at low CSNRs, but worsen the performance at high CSNRs. We remark on this phenomenon from two points of view. On the one hand, at high average CSNR, the system performance is already reached its floor value; hence, the system performance will be affected more by the five relatively low CSNR links rather than the five relatively high CSNR links. So, the deviation between link noises can only worsen the overall performance. On the other hand, the error control coding technique used allows the fusion center to make the correct global decision even if there are several faulty sensors. Therefore, by sacrificing the local CSNR of some sensors to increase the local CSNR of the remaining sensors (so that the overall average CSNR is fixed), the system performance can be improved.

In Fig. 6.48, since the system is simulated at high CSNR=10 dB, the unbalance in local noise variances will slightly worsen the performance.

Repeating the above simulations with 3×10 and 5×10 code matrices under $\rho = 0.1$ and 0.9 yields Figs. 6.49–6.64, for which similar remarks can be accordingly made.

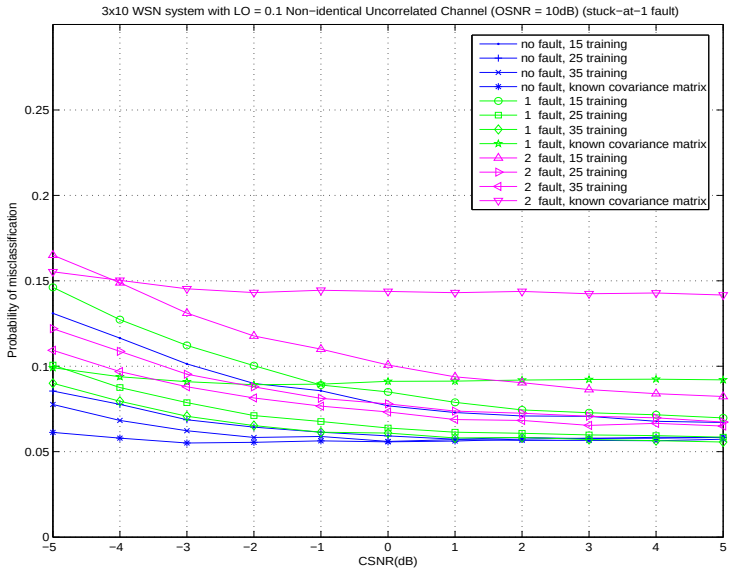

Figure 6.49: Performance of the MED rule under $\rho = 0.1$ non-identical uncorrelated channel at OSNR=10 dB for stuck-at-1 faults when 3×10 code matrix is employed.

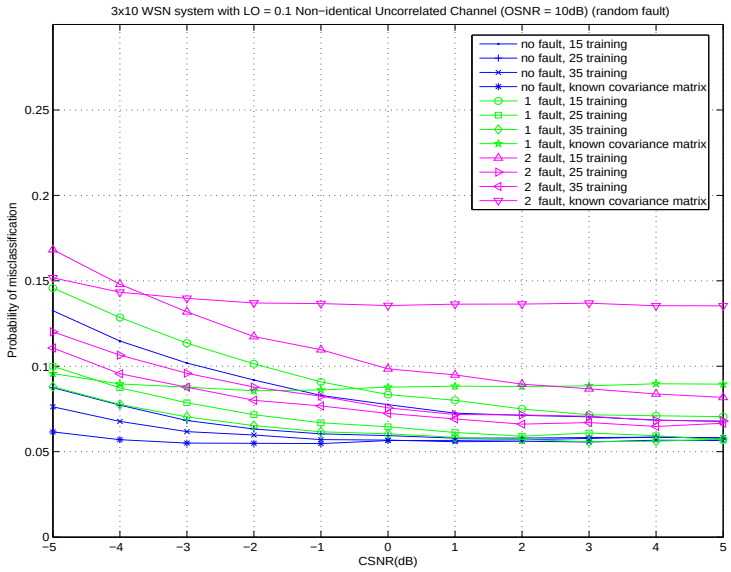

Figure 6.50: Performance of the MED rule under $\rho = 0.1$ non-identical uncorrelated channel at OSNR=10 dB for random faults when 3×10 code matrix is employed.

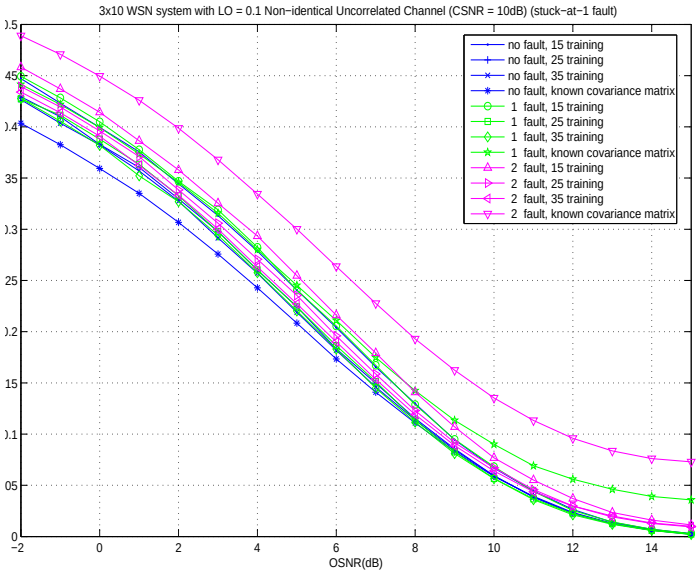

Figure 6.51: Performance of the MED rule under $\rho = 0.1$ non-identical uncorrelated channel at CSNR=10 dB for stuck-at-1 faults when 3×10 code matrix is employed.

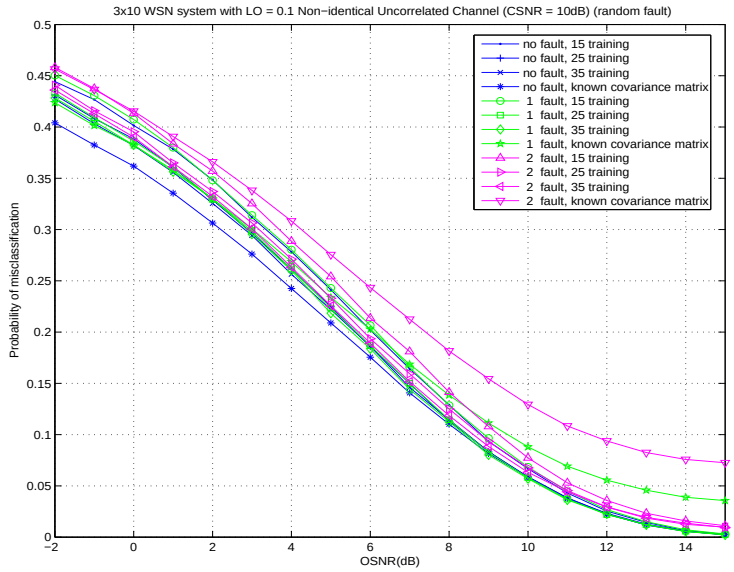

Figure 6.52: Performance of the MED rule under $\rho = 0.1$ non-identical uncorrelated channel at CSNR=10 dB for random faults when 3×10 code matrix is employed.

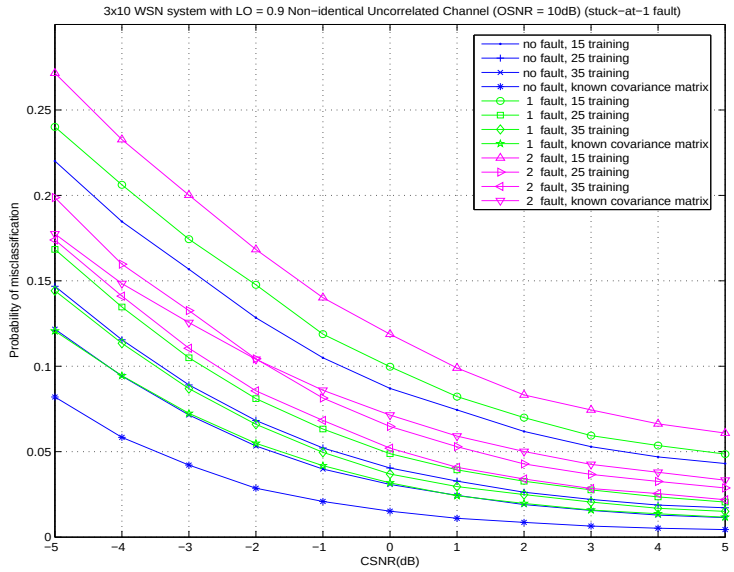

Figure 6.53: Performance of the MED rule under $\rho = 0.9$ non-identical uncorrelated channel at OSNR=10 dB for stuck-at-1 faults when 3×10 code matrix is employed.

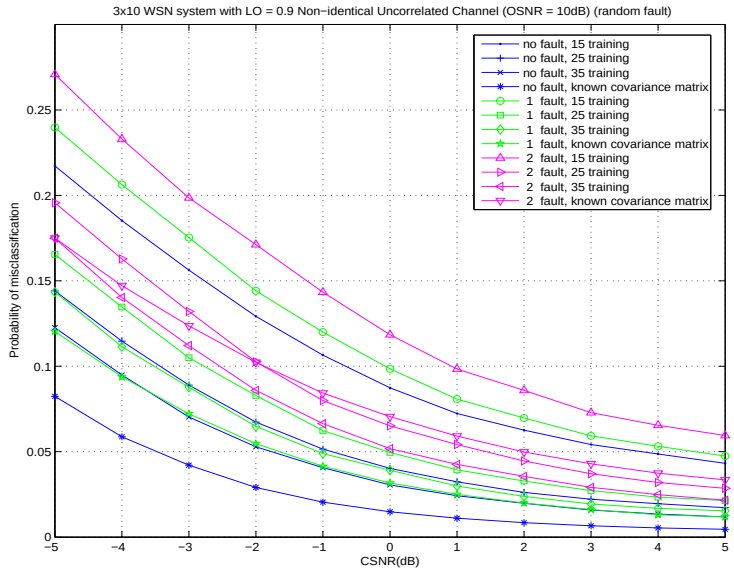

Figure 6.54: Performance of the MED rule under $\rho = 0.9$ non-identical uncorrelated channel at OSNR=10 dB for random faults when 3×10 code matrix is employed.

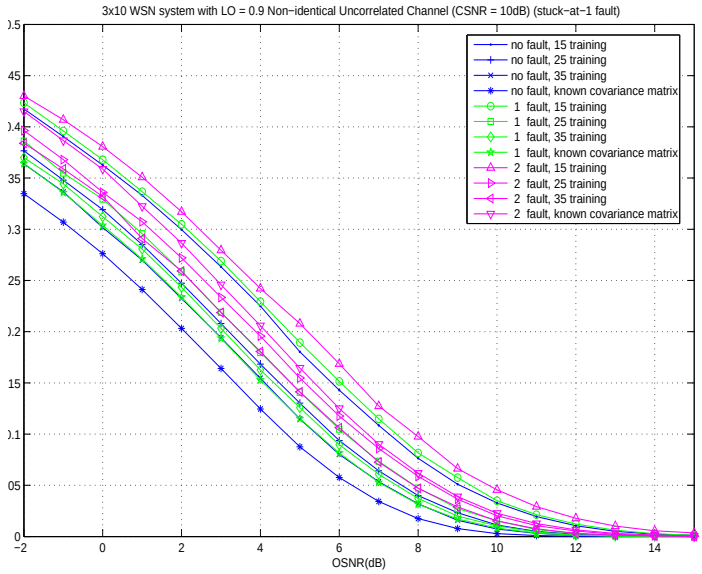

Figure 6.55: Performance of the MED rule under $\rho = 0.9$ non-identical uncorrelated channel at CSNR=10 dB for stuck-at-1 faults when 3×10 code matrix is employed.

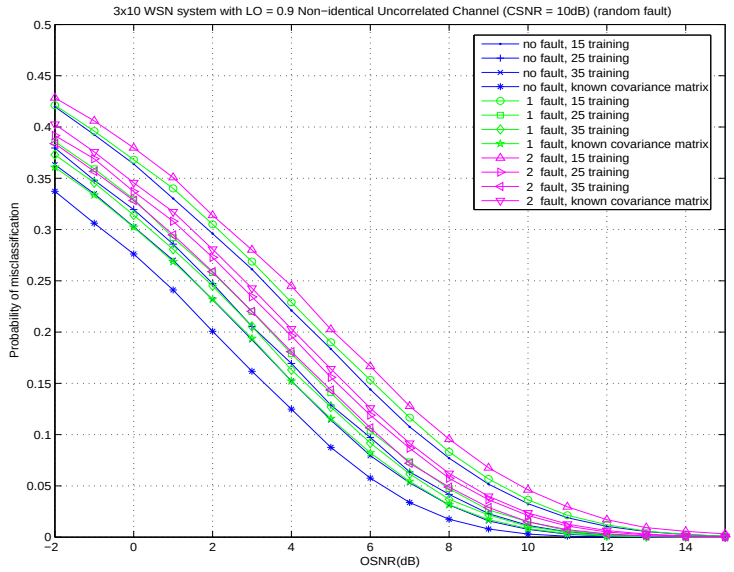

Figure 6.56: Performance of the MED rule under $\rho = 0.9$ non-identical uncorrelated channel at CSNR=10 dB for random faults when 3×10 code matrix is employed.

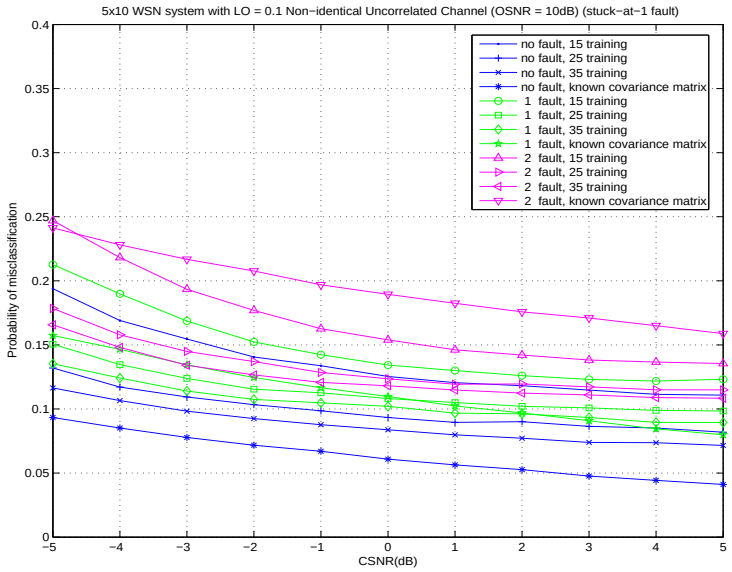

Figure 6.57: Performance of the MED rule under $\rho = 0.1$ non-identical uncorrelated channel at OSNR=10 dB for stuck-at-1 faults when 5×10 code matrix is employed.

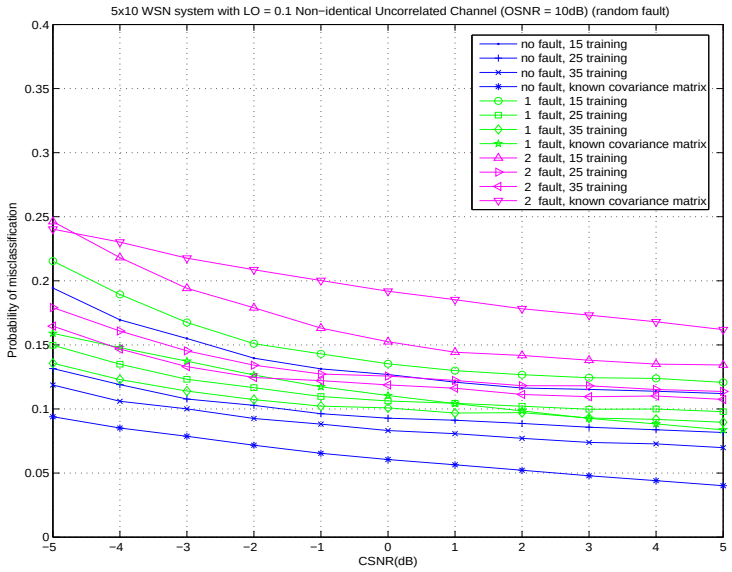

Figure 6.58: Performance of the MED rule under $\rho = 0.1$ non-identical uncorrelated channel at OSNR=10 dB for random faults when 5×10 code matrix is employed.

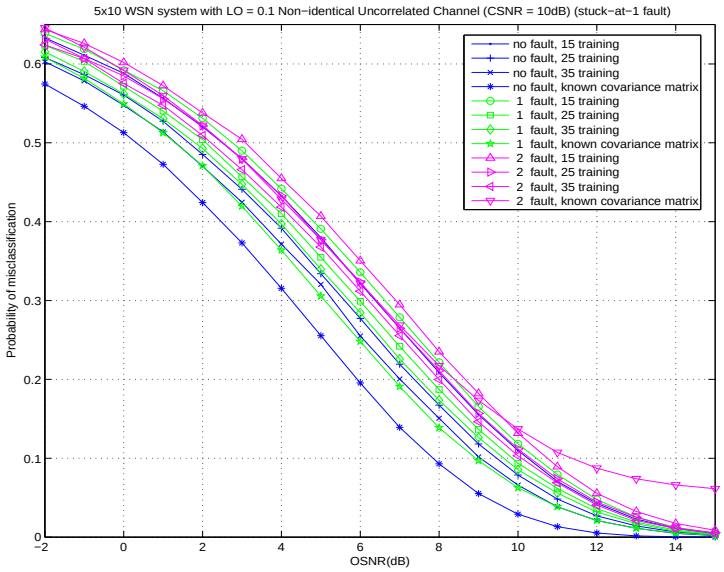

Figure 6.59: Performance of the MED rule under $\rho = 0.1$ non-identical uncorrelated channel at CSNR=10 dB for stuck-at-1 faults when 5×10 code matrix is employed.

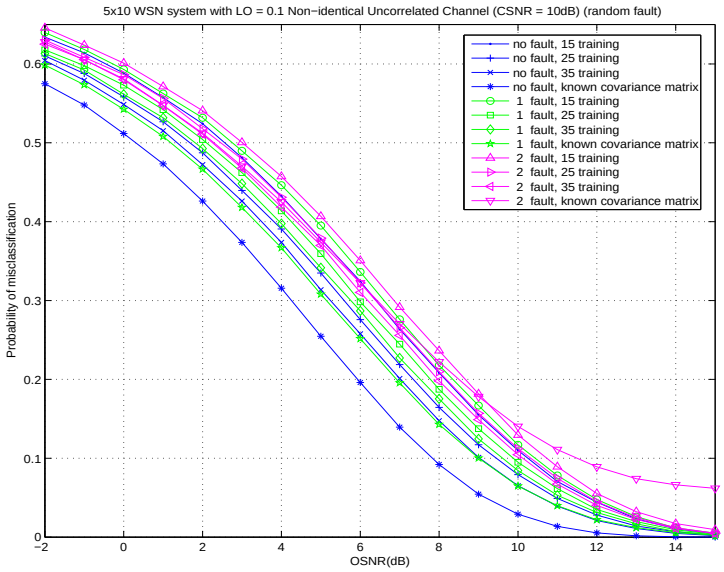

Figure 6.60: Performance of the MED rule under $\rho = 0.1$ non-identical uncorrelated channel at CSNR=10 dB for random faults when 5×10 code matrix is employed.

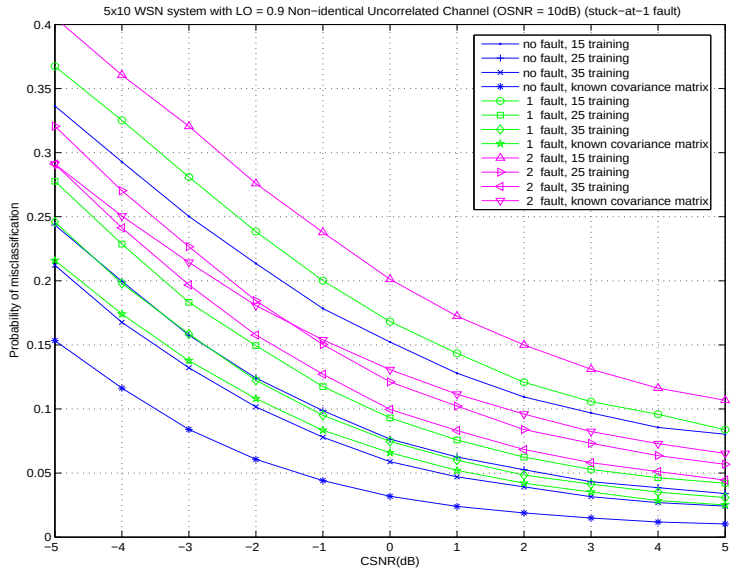

Figure 6.61: Performance of the MED rule under $\rho = 0.9$ non-identical uncorrelated channel at OSNR=10 dB for stuck-at-1 faults when 5×10 code matrix is employed.

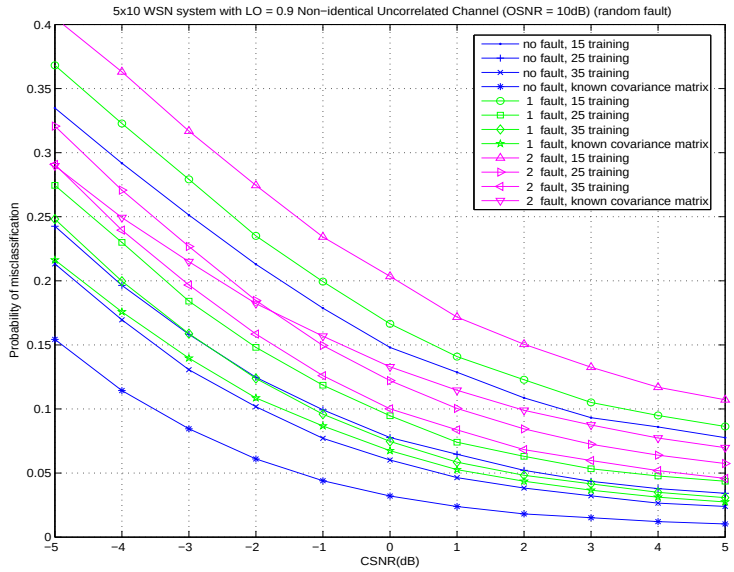

Figure 6.62: Performance of the MED rule under $\rho = 0.9$ non-identical uncorrelated channel at OSNR=10 dB for random faults when 5×10 code matrix is employed.

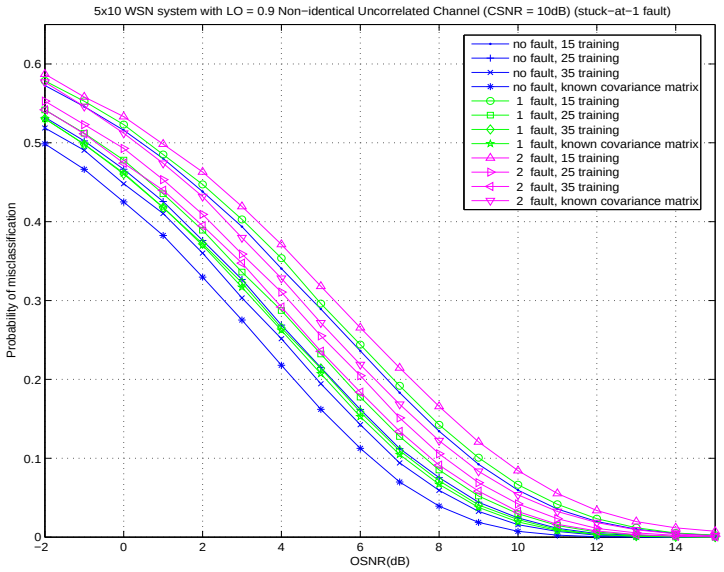

Figure 6.63: Performance of the MED rule under $\rho = 0.9$ non-identical uncorrelated channel at CSNR=10 dB for stuck-at-1 faults when 5×10 code matrix is employed.

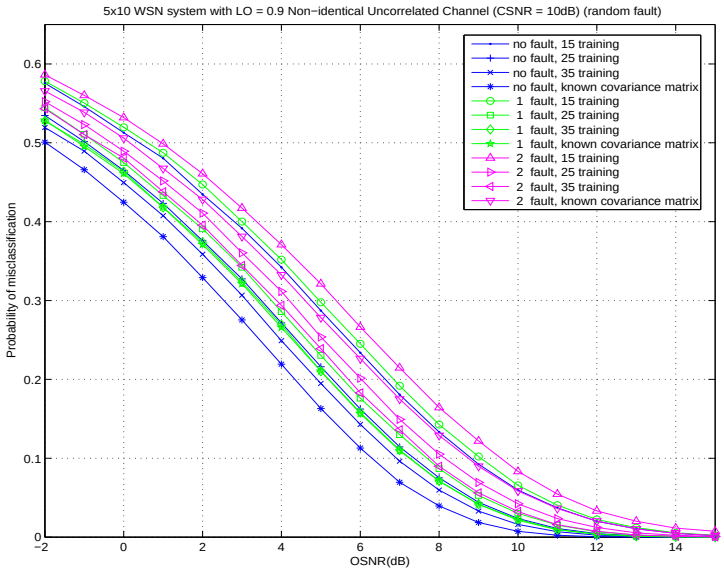

Figure 6.64: Performance of the MED rule under $\rho = 0.9$ non-identical uncorrelated channel at CSNR=10 dB for random faults when 5×10 code matrix is employed.

Chapter 7

Conclusion

In this thesis, we propose a soft-decision fusion rule to be employed in the WSN classification system under correlated additive Gaussian link noises. In light of the DCFECC approach, the minimum Euclidean distance (MED) fusion rule successfully provides a considerable fault-tolerance capability against both deterministic or random sensor faults. With the help of the pre-sent training sequence, the channel covariance matrix can be maximum-likelihoodly estimated, and further optimally equalized by means of the modified MED fusion rule. Furthermore, in terms of the MED fusion rule, the code matrix search criterion can be simplified under AWGN channel assumption.

BIBLIOGRAPHY

[1] I. F. Akyildiz, W. Su, Y. Sankarasubramaniam, and E. Cayirci, "A survey on sensor networks," *IEEE Communications Magazine*, pp. 102-114, August 2002.

[2] L. Dan, K. D. Wong, H. H. Yu, and A. M. Sayeed, "Detection, classification, and tracking of targets," *IEEE Signal Processing Magazine*, vol. 19, pp. 17-29, March 2002.

[3] H. Wang, J. Elson, L. Girod, D. Estrin, and K. Yao, "Target classification and localization in habitat monitoring," in *IEEE International Conference on Acoustics, Speech, and Signal Processing (ICASSP 2003)*, vol. 4, Hong Kong, China, April 2003, pp. 844-847.

[4] S. A. Aldosari and J. M. F. Moura, "Detection in decentralized sensor networks," in *IEEE International Conference on Acoustics, Speech, and Signal Processing*, Montreal, Canada, May 2004, pp. 277-280.

[5] A. D'Costa and A. M. Sayeed, "Data versus decision fusion in sensor networks," in *IEEE International Conference on Acoustics, Speech, and Signal Processing*, Hong Kong, China, April 2003, pp. 832-835.

[6] A. D'Costa and A. M. Sayeed, "Data versus decision fusion for classification in sensor networks," in *The 6th International Conference on Information Fusion*, Cains, Australia, July 2003, pp. 889-894.

[7] T.-Y. Wang, Y. S. Han, P. K. Varshney, and P.-N. Chen, "Distributed fault-tolerant classification in wireless sensor networks," *IEEE Journal of Selected Areas in Communications*, vol. 23, no. 4, pp. 724-734, April 2005.

[8] P.-N. Chen, T.-Y. Wang, Y. S. Han, P. K. Varshney, and C. Yao, "Performance analysis and code design for minimum hamming distance fusion in wireless sensor networks," *submitted to IEEE Trans. Inform. Theory*, November 2005.

[9] T.-Y. Wang, Y. S. Han, B. Chen, and P. K. Varshney, "A combined decision fusion and channel coding scheme for distributed fault-tolerant classification in wireless sensor networks," *IEEE Trans. Wireless Commun.*, to appear.